A local moment approach to the Anderson model

1998 J. Phys.: Condens. Matter 10 2673

(http://iopscience.iop.org/0953-8984/10/12/009)

J. Phys.: Condens. Matter **10** (1998) 2673–2700. Printed in the UK PII: S0953-8984(98)90661-0

A local moment approach to the Anderson model

David E Logan, Michael P Eastwood and Michael A Tusch

Oxford University, Physical and Theoretical Chemistry Laboratory, South Parks Road, Oxford OX1 3QZ, UK

Received 13 January 1998

Abstract. A theory is developed for the single-particle spectra of the symmetric Anderson model, in which local moments are introduced explicitly from the outset. Dynamical coupling of single-particle processes to low-energy spin-flip excitations leads, within the framework of a two-self-energy description, to a theory in which both low- and high-energy spectral features are simultaneously captured, while correctly preserving Fermi liquid behaviour at low energies. The atomic limit, non-interacting limit and strong-coupling behaviour of the spectrum are each recovered. For strong coupling in particular, both the exponential asymptotics of the Kondo resonance and concomitant many-body broadening of the Hubbard satellite bands are shown to arise naturally within the present approach.

1. Introduction

The single-impurity Anderson model [1] has long served as a paradigm for the understanding of magnetic impurities in metals, and more generally as a generic model for the physics of strong, local electron correlations [2]. Thermodynamic and low-energy properties of the model are by now well understood, in particular from Bethe *ansatz* [3] and renormalization group [4] studies. But despite much important work in recent years (reviewed comprehensively in [2]), the situation is much less satisfactory as far as dynamics, and in particular spectral functions, are concerned.

In this paper we consider the symmetric, spin-$\frac{1}{2}$ Anderson model; and seek to develop a theory for its single-particle spectra as a function of the local interaction strength U. Ideally, a satisfactory description of such should have the following characteristics.

(i) It should be capable of describing simultaneously both low- and high-energy spectral features: the Kondo resonance and the Hubbard satellite bands respectively.

(ii) Fermi liquid behaviour should be recovered correctly at low energies, in particular the quasiparticle form for the impurity Green function.

(iii) The atomic limit, non-interacting limit ($U = 0$) and strong-coupling ($U \to \infty$) behaviour of the spectrum should all be encompassed.

For strong coupling in particular, the exponential diminution of the Kondo scale with interaction strength, $\ln \omega_{\mathrm{K}} \propto -U$, should be captured; together with concomitant many-body spectral broadening of the satellite bands.

While desirable, the above aims are by no means straightforward to achieve in practice. To describe high-energy spectral properties, particularly in strong coupling, an expansion in the host–impurity hybridization, starting from the atomic limit, is natural. This underlies for example both $1/N$ expansions [5–7] (with N the impurity degeneracy) and the non-crossing approximation [8–11]. These approaches are designed to capture the $N \to \infty$

0953-8984/98/122673+28$19.50

limit (as opposed to the spin-$\frac{1}{2}$ case, $N = 2$), and are most successful in the extreme asymmetric limit with $U = \infty$. While high-energy excitations are in general rather well described by such, they are unsatisfactory at low energies where Fermi liquid behaviour is violated; similar comments apply to their finite-U generalizations (see e.g. [6, 11]), where in addition the non-interacting limit is not recovered. Slave boson methods [12–14], by contrast, are designed to handle low energies and capture Fermi liquid behaviour, again most successfully in the large-N and extreme asymmetric limits. Their ability to describe high-energy properties is however much less satisfactory. Further, due to the difficulties of handling double occupancy, extension to finite U is not straightforward; progress in this regard (see e.g. [14]) is confined in practice to large degeneracies, and cannot capture the spin-degenerate case $N = 2$.

An alternative is finite-order perturbation theory in U about the non-interacting limit [15, 16]. The full spectrum is thereby obtained and, at least for the symmetric Anderson model, Fermi liquid behaviour arises straightforwardly. But the approach is limited to weak/moderate interaction strengths; strong-coupling spectral asymptotics, and in particular the exponentiality of the Kondo scale, cannot be described. Variants of it, involving self-consistent renormalization and/or partial resummation, have met with mixed success (see e.g. [17]) and are again restricted in practice to weak/moderate interactions.

While much has been learnt from all of the above approaches, it is clear from the brief discussion given that there is a need for the development of further, necessarily approximate, many-body theories; particularly in the strong-coupling regime. One such is described in this paper. We begin with an underlying mean-field theory and its associated spin fluctuations; single-particle processes are then coupled dynamically to low-energy spin excitations, leading to a many-body description of the single-particle spectra. In this sense, our approach is quite conventional. But it is unconventional in that, as in Anderson's original seminal paper [1], the 'zeroth-order' mean-field approach from which we start is unrestricted Hartree–Fock (UHF), in which the notion of an impurity local moment enters explicitly from the outset. The deficiencies of this simple mean-field approximation *per se* are sufficiently severe that there have been few attempts to use it as the basis for a genuine many-body theory. In section 2 of this paper, however, we argue that the specific nature of its deficiencies, particularly with regard to associated spin fluctuations in the transverse spin channel, suggest what is required to successfully transcend it. This is considered explicitly in section 3 via a 'two-self-energy' description of the impurity Green functions; and with a specific approximation employed for the self-energies that is motivated on physical grounds, since it captures the dynamical spin-flip scattering required in particular to describe the Kondo, or spin-fluctuation, limit.

The desiderata outlined above are quite satisfactorily achieved by the resultant theory. In section 4 the strong-coupling behaviour of the impurity spectrum is established analytically. We consider first the spectral asymptotics at low energies, in particular the origin and U-dependence of the Kondo scale and the emergence of Fermi liquid behaviour; and then, in close parallel, the corresponding asymptotic behaviour of the high-energy satellite bands. From the former, the further physical significance of the Kondo scale within the present approach is also apparent, in that it sets the timescale ($\sim 1/\omega_{\mathrm{K}}$) for restoration of the locally broken symmetry inherent in the zeroth-order mean-field level of description.

While our general analysis assumes only that the host is metallic, with a symmetric hybridization function, we consider in section 5 the particular, common case of a flat-band host. Illustrative spectra are shown, including the low-energy scaling behaviour as the spin-fluctuation limit is approached; the role of additional scattering processes is considered

briefly; and two simple, heuristic extensions are described that serve further to illustrate the generality of the underlying approach. The paper concludes with a brief summary.

2. Motivation

With the Fermi level taken as the energy origin, the Hamiltonian for the spin-$\frac{1}{2}$ Anderson model is given in standard notation by

$$\hat{H} = \hat{H}_{\text{host}} + \hat{H}_{\text{impurity}} + \hat{H}_{\text{hybridization}} \tag{2.1}$$

$$= \sum_{\boldsymbol{k},\sigma} \epsilon_{\boldsymbol{k}} \hat{n}_{\boldsymbol{k}\sigma} + \sum_{\sigma} \left(\epsilon_i + \frac{U}{2} \hat{n}_{i-\sigma} \right) \hat{n}_{i\sigma} + \sum_{\boldsymbol{k},\sigma} V_{i\boldsymbol{k}} (c^{\dagger}_{i\sigma} c_{\boldsymbol{k}\sigma} + c^{\dagger}_{\boldsymbol{k}\sigma} c_{i\sigma}) \tag{2.2}$$

with $\epsilon_{\boldsymbol{k}}$ the host dispersion, $V_{i\boldsymbol{k}}$ the hybridization and ϵ_i the impurity level; for the symmetric Anderson model considered here, $\epsilon_i = -U/2$ with U the on-site interaction.

We consider the zero-temperature single-particle impurity Green function, defined by

$$G(t) = -\mathrm{i} \left\langle T\{c_{i\sigma}(t) c^{\dagger}_{i\sigma}\} \right\rangle = G^{+}(t) + G^{-}(t) \tag{2.3}$$

and separated for later purposes into retarded ($+$, $t > 0$) and advanced ($-$, $t \leqslant 0$) components; since $\hat{H}$ is invariant under $\sigma \to -\sigma$ ('up–down spin symmetry'), G is naturally independent of spin, σ. In the non-interacting limit, where $\epsilon_i = -U/2 = 0$, the Green function is given by

$$g(\omega) = [\omega + \mathrm{i}\eta \,\mathrm{sgn}(\omega) - \Delta(\omega)]^{-1} \qquad \eta \to 0^{+} \tag{2.4}$$

with hybridization function

$$\Delta(\omega) = \sum_{\boldsymbol{k}} \frac{|V_{i\boldsymbol{k}}|^2}{\omega - \epsilon_{\boldsymbol{k}} + \mathrm{i}\eta \,\mathrm{sgn}(\omega)} \tag{2.5a}$$

$$= \Delta_{\mathrm{R}}(\omega) - \mathrm{i}\,\mathrm{sgn}(\omega) \Delta_{\mathrm{I}}(\omega). \tag{2.5b}$$

We consider throughout a symmetric hybridization, $\Delta(\omega) = -\Delta(-\omega)$, such that

$$\Delta_{\mathrm{R}}(\omega) = -\Delta_{\mathrm{R}}(-\omega) \tag{2.6a}$$

$$\Delta_{\mathrm{I}}(\omega) = \Delta_{\mathrm{I}}(-\omega) = \Delta_0 + \mathcal{O}(\omega^2) \tag{2.6b}$$

where Δ_0 is thus defined quite generally; the usual flat-band model [2] with infinite bandwidth ($D \to \infty$) is a particular case of equation (2.6), for which $\Delta_{\mathrm{R}}(\omega) = 0$ and $\Delta_{\mathrm{I}}(\omega) = \Delta_0$ for all ω.

From particle–hole symmetry the Fermi level remains pinned at $\omega = 0$ for all $U \geqslant 0$; likewise the impurity charge $n_i = \sum_{\sigma} \langle \hat{n}_{i\sigma} \rangle = 1 \ \forall U$. The impurity Green function $G(\omega) = X(\omega) - \mathrm{i}\pi \,\mathrm{sgn}(\omega) D(\omega)$ ($= -G(-\omega)$ by particle–hole symmetry) may be written as

$$G(\omega) = [\omega + \mathrm{i}\eta \,\mathrm{sgn}(\omega) - \Delta(\omega) - \Sigma(\omega)]^{-1} \tag{2.7}$$

where the (local) interaction self-energy

$$\Sigma(\omega) = \Sigma_{\mathrm{R}}(\omega) - \mathrm{i}\,\mathrm{sgn}(\omega) \Sigma_{\mathrm{I}}(\omega) \tag{2.8}$$

such that $\Sigma(\omega) = -\Sigma(-\omega)$, is defined by equation (2.7) and excludes the trivial Hartree contribution (of $(U/2)n_i = U/2$, which cancels $\epsilon_i = -U/2$). For Fermi liquid behaviour to be satisfied, $\Sigma_{\mathrm{I}}(\omega) \sim \mathcal{O}(\omega^2)$ as $\omega \to 0$, and from equation (2.7) the low-ω behaviour of $G(\omega)$ thus takes the familiar quasiparticle form

$$G(\omega) = \frac{Z}{\omega + \mathrm{i}\,\mathrm{sgn}(\omega) Z(\Delta_0 + \mathcal{O}(\omega^2))} \tag{2.9a}$$

in terms of the quasiparticle weight

$$Z = \left[1 - \left(\frac{\partial}{\partial\omega}[\Sigma_{\rm R}(\omega) + \Delta_{\rm R}(\omega)]\right)_{\omega=0}\right]^{-1} \tag{2.9b}$$

which in strong coupling is proportional to the Kondo scale, $Z \propto \omega_{\rm K}$. From (2.9*a*) follows directly a well known result [2] that proves important in our subsequent theory: $G(\omega = 0) = g(\omega = 0)$, whence the single-particle spectrum is pinned at the Fermi level; that is

$$D(\omega = 0) = (\pi\Delta_0)^{-1} \qquad \forall U. \tag{2.10}$$

Equation (2.9*a*) forms a starting point for microscopic Fermi liquid theory (see e.g. [2]), and is naturally applicable on the lowest energy scales relevant to the Kondo resonance. But by itself, of course, and granted even a knowledge of $Z \propto \omega_{\rm K}$, it says nothing about the high-energy single-particle excitations embodied in the Hubbard bands, whose characteristics are in turn closely related to the existence of the low-ω Kondo scale (see sections 2.1, 4.2). For this a theory is required that simultaneously covers all energy scales, while reproducing correctly the low-frequency quasiparticle form, equation (2.9*a*). Finite-order perturbation theory in U about the non-interacting limit [15, 16] is an obvious candidate, but is well known to be unable to describe the exponential strong-coupling asymptotics of the Kondo scale. A somewhat more radical approach is perhaps required.

2.1. Mean field

As known since Anderson's original paper [1], unrestricted Hartree–Fock (UHF) is the simplest (indeed only) mean-field approximation in which the notion of an impurity local moment (μ_i), regarded as the first effect of electron interactions and determined self-consistently, enters explicitly from the outset: $\mu_i = \langle\hat{n}_{i\uparrow} - \hat{n}_{i\downarrow}\rangle_0$, with $\langle\cdots\rangle_0$ an average over the mean-field ground state. There are two reasons for first considering this simple approximation, and its associated spin fluctuations (section 2.2). First, rather prosaically, because the UHF Green functions essentially form the bare propagators for our subsequent theory. The second relates to its deficiencies. These are well known for *restricted* Hartree–Fock (RHF, where $\mu_i = 0$ is enforced for all U); but are quite different for UHF, careful scrutiny of which suggests what is required to circumvent its limitations.

The essential feature of UHF is that, when local moments exist, two degenerate self-consistent solutions are possible: $\mu_i = +|\mu|$ and $-|\mu|$. Accordingly, the total σ-spin Green function is given by

$$G^0(\omega) = \frac{1}{2}[\mathcal{G}_{{\rm A}\sigma}(\omega) + \mathcal{G}_{{\rm B}\sigma}(\omega)] \tag{2.11}$$

reflecting the equal probability with which the moment may be found up ('A', $\mu_i = +|\mu|$) as down ('B'); and where, with α = A or B and $\sigma = +/-$ for $\uparrow/\downarrow$ spins, the $\mathcal{G}_{\alpha\sigma}(\omega) = {\rm Re}\,\mathcal{G}_{\alpha\sigma}(\omega) - {\rm i}\pi\,{\rm sgn}(\omega)D^0_{\alpha\sigma}(\omega)$ are given by

$$\mathcal{G}_{\alpha\sigma}(\omega) = \left[\omega + {\rm i}\eta\,{\rm sgn}(\omega) - \Delta(\omega) - \tilde{\Sigma}^0_{\alpha\sigma}(\omega)\right]^{-1} \tag{2.12a}$$

with UHF interaction self-energies

$$\tilde{\Sigma}^0_{{\rm A}\sigma}(\omega) = -\frac{\sigma}{2}U|\mu| = -\tilde{\Sigma}^0_{{\rm B}\sigma}(\omega). \tag{2.12b}$$

The corresponding spectral densities are thus simply

$$D^0_{{\rm A}\sigma}(\omega) = \frac{\Delta_{\rm I}(\omega)\pi^{-1}}{[\omega + (\sigma/2)U|\mu| - \Delta_{\rm R}(\omega)]^2 + [\Delta_{\rm I}(\omega)]^2} \tag{2.12c}$$

(and analogously for $D^0_{B\sigma}(\omega)$), representing essentially the UHF approximations to the lower ($\sim D^0_{A\uparrow}(\omega)$) and upper ($\sim D^0_{A\downarrow}(\omega)$) Hubbard satellites; in the flat-band case, they are simple Lorentzians of half-width Δ_0, centred on $\omega = \mp\frac{1}{2}U|\mu|$.

There are two important basic symmetries, namely

$$D^0_{A\sigma}(\omega) = D^0_{B-\sigma}(\omega) \tag{2.13a}$$

$$= D^0_{A-\sigma}(-\omega) \tag{2.13b}$$

reflecting respectively up–down spin symmetry ($\mathcal{G}_{A\sigma}(\omega) = \mathcal{G}_{B-\sigma}(\omega)$) and particle–hole symmetry ($\mathcal{G}_{\alpha\sigma}(\omega) = -\mathcal{G}_{\alpha-\sigma}(-\omega)$). From the former it follows that $G^0(\omega)$ (equation (2.11)) is correctly independent of spin, σ; while from the latter,

$$G^0(\omega) = -G^0(-\omega). \tag{2.14}$$

The UHF equations are naturally closely related to those of the so-called alloy analogy approximation (AAA) arising to lowest order in an equation-of-motion approach (see e.g. [18]), but with one exception: in the AAA, equations (2.11)–(2.14) hold but with the impurity local moment $|\mu| = 1\ \forall U$, while for UHF by contrast $|\mu|$ is determined self-consistently from

$$|\mu| = \int_{-\infty}^{0} d\omega\ [D^0_{A\uparrow}(\omega) - D^0_{A\downarrow}(\omega)]. \tag{2.15}$$

For the flat-band case, this is given explicitly by

$$|\tilde{\mu}| = \tan^{-1}(\tilde{U}|\tilde{\mu}|) \tag{2.16a}$$

where

$$\tilde{U} = U/\pi\Delta_0 \qquad |\tilde{\mu}| = \frac{\pi}{2}|\mu|. \tag{2.16b}$$

$\tilde{U}$ is the reduced (dimensionless) interaction strength. From equation (2.16*a*), $\tilde{U}_c = 1$ is the boundary to impurity local moment formation: for $\tilde{U} < 1$, $|\mu| = 0$ is the sole solution, and UHF coincides with RHF. For $\tilde{U} > 1$ the self-consistent $|\mu|$ increases quite rapidly with $\tilde{U}$—the impurity moment is well developed by $\tilde{U} \sim 2$ (where $|\mu| \sim 3/4$)—and $|\mu| \to 1$ in strong coupling, $\tilde{U} \to \infty$, where the AAA is recovered.

Although both the atomic limit ($\Delta_0 = 0$) and the non-interacting limit are correctly recovered by UHF, the deficiencies of the approximation are of course severe: for $\tilde{U} < 1$ the Green function is trivially $\tilde{U}$-independent and coincides with the non-interacting limit; more significantly, for $\tilde{U} > 1$ Fermi liquid behaviour is violated and there is no hint of a low-frequency Kondo resonance. The latter is inevitable for any inherently static approximation with an ω-independent self-energy $\tilde{\Sigma}_{\alpha\sigma}$ (as in equation (2.12*b*)), since the essence of Fermi liquid behaviour is the inelasticity of electron scattering near the Fermi level, $\omega = 0$.

The virtue of UHF is that it describes the high-energy Hubbard satellites, centred on $\omega \sim \pm U/2$ in strong coupling. Yet even here it is unsatisfactory, as shown by a simple physical argument (illustrated for simplicity with reference to the flat-band case). Consider the upper Hubbard band (UHB) in strong coupling, and imagine adding an $\uparrow$-spin electron to a $\downarrow$-spin occupied (B-type) impurity. UHF is a static approximation, whence only the added $\uparrow$ spin can hop, its rate of loss from the impurity site being Δ_0. Thus, the UHF result for the UHB is

$$G^0(\omega) \simeq \frac{1}{2}\mathcal{G}_{B\uparrow}(\omega) \sim \frac{1/2}{(\omega - U/2) + i\Delta_0} \qquad \text{UHF} \tag{2.17a}$$

(as follows directly from equations (2.11), (2.12)), leading to a Lorentzian band of width Δ_0. But in reality, having added an $\uparrow$-spin electron to a $\downarrow$-spin occupied impurity, the $\downarrow$ spin

itself can clearly hop off the site, leaving behind a spin flip on the impurity. The energy cost for the spin flip is of the order of the Kondo scale ω_K which, being exponentially small in strong coupling, is immaterially small on the scale $\omega \sim U/2 \gg \omega_K$ appropriate to the UHB: the $\downarrow$-spin electron itself thus has a loss rate Δ_0, the total loss rate from the site is then $2\Delta_0$, whence

$$G(\omega) \simeq \frac{1/2}{(\omega - U/2) + 2i\Delta_0} \tag{2.17b}$$

(and analogously for the lower Hubbard band), producing a Lorentzian Hubbard satellite of width $2\Delta_0$. The occurrence of additional spectral broadening is well known (see e.g. [11]), but its physical origin is evidently simple and closely connected to the existence of the low-frequency spin-flip scale. While a static approximation such as UHF cannot describe the additional many-body broadening, it is clear from the simple physical considerations above what is required to transcend it: single-particle processes must be coupled dynamically to low-frequency spin fluctuations. We consider first the latter.

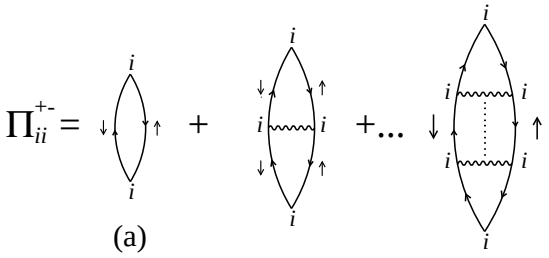

Figure 1. Particle–hole ladder sum in the transverse spin channel, for Π^{+-}_{ii}. Bare propagators are denoted by solid lines, the on-site interactions by wiggles. For Π^{-+}_{ii}, the spins are reversed.

2.2. Spin fluctuations

2.2.1. Propagator for transverse spin excitations. We focus on spin fluctuations in the transverse spin channel, reflected in the polarization propagators $\Pi^{+-}_{ii}(t) = i\langle T\{S^+_i(t)S^-_i\}\rangle$ and $\Pi^{-+}_{ii}(t)$. These are given at the simplest level of approximation by the ladder sum of repeated particle–hole interactions shown in figure 1; bare UHF propagators are denoted by solid lines, and the on-site interaction (conserving spin at each vertex end) by a wiggly line. The bare polarization bubble, diagram (a) in figure 1, is given explicitly by

$${}^0\Pi^{+-}_{\alpha\alpha}(\omega) = i\int_{-\infty}^{\infty} \frac{d\omega_1}{2\pi}\, \mathcal{G}_{\alpha\downarrow}(\omega_1)\mathcal{G}_{\alpha\uparrow}(\omega_1 - \omega) \tag{2.18}$$

(where $\alpha =$ A or B); the corresponding ${}^0\Pi^{-+}_{\alpha\alpha}(\omega)$ bubble follows simply by interchanging the spin labels, $\uparrow \leftrightarrow \downarrow$, in equation (2.18). Note that the four transverse spin-polarization bubbles coincide only for $|\mu| = 0$; in general, for $|\mu| \neq 0$, they are distinct, although related by the following symmetries. From up–down spin symmetry (equation (2.13*a*)) it follows directly that

$${}^0\Pi^{+-}_{\alpha\alpha}(\omega) = {}^0\Pi^{-+}_{\bar\alpha\bar\alpha}(\omega) \tag{2.19a}$$

where $\bar\alpha =$ B or A for $\alpha =$ A or B respectively; while a simple change of variables in equation (2.18) gives

$${}^0\Pi^{+-}_{\alpha\alpha}(\omega) = {}^0\Pi^{-+}_{\alpha\alpha}(-\omega). \tag{2.19b}$$

From equations (2.19), only ${}^0\Pi^{+-}_{AA}$ need be considered: the remaining ${}^0\Pi$s follow from it. The ladder sum of figure 1 is given simply by the RPA form

$$\Pi^{+-}_{\alpha\alpha}(\omega) = {}^0\Pi^{+-}_{\alpha\alpha}(\omega)/(1 - U^0\Pi^{+-}_{\alpha\alpha}(\omega)) \tag{2.20}$$

to which the symmetries in equation (2.19) likewise apply. And the real/imaginary parts of both the ${}^0\Pi$s and Πs are related via the Hilbert transform

$$\Pi^{+-}_{\alpha\alpha}(\omega) = \int_{-\infty}^{\infty} \frac{d\omega_1}{\pi} \frac{\operatorname{Im}\Pi^{+-}_{\alpha\alpha}(\omega_1)\operatorname{sgn}(\omega_1)}{\omega_1 - \omega - i\eta\operatorname{sgn}(\omega_1)} \tag{2.21a}$$

in particular,

$$\operatorname{Re}\Pi^{+-}_{\alpha\alpha}(\omega = 0) = \int_{-\infty}^{\infty} \frac{d\omega_1}{\pi} \frac{\operatorname{Im}\Pi^{+-}_{\alpha\alpha}(\omega_1)}{|\omega_1|} > 0 \tag{2.21b}$$

the positivity of which follows since $\operatorname{Im}\Pi^{+-}_{\alpha\alpha}(\omega) \geqslant 0$.

The low-frequency behaviour of $\Pi^{+-}_{AA}(\omega)$ follows from that of ${}^0\Pi^{+-}_{AA}(\omega)$. From equation (2.18), using $\mathcal{G}_{\alpha\sigma}(\omega) = \mathcal{G}^+_{\alpha\sigma}(\omega) + \mathcal{G}^-_{\alpha\sigma}(\omega)$ and the Hilbert transform

$$\mathcal{G}^{\pm}_{\alpha\sigma}(\omega) = \int_{-\infty}^{\infty} d\omega_1 \frac{D^0_{\alpha\sigma}(\omega_1)\theta(\pm\omega_1)}{\omega - \omega_1 \pm i\eta} \tag{2.22}$$

(with $\theta(\omega)$ the unit step function), a simple calculation gives

$$\begin{aligned}\frac{1}{\pi}\operatorname{Im}{}^0\Pi^{+-}_{AA}(\omega) = {}&\theta(\omega)\int_0^{|\omega|} d\omega_1\ D^0_{A\downarrow}(\omega_1)D^0_{A\uparrow}(\omega_1 - \omega)\\ &+ \theta(-\omega)\int_{-|\omega|}^{0} d\omega_1\ D^0_{A\downarrow}(\omega_1)D^0_{A\uparrow}(\omega_1 - \omega).\end{aligned} \tag{2.23a}$$

Thus, since $D^0_{\alpha\sigma}(\omega = 0)$ is non-vanishing at the Fermi level,

$$\frac{1}{\pi}\operatorname{Im}{}^0\Pi^{+-}_{AA}(\omega) \overset{\omega\to 0}{\sim} |\omega| D^0_{A\downarrow}(0)D^0_{A\uparrow}(0) \tag{2.23b}$$

vanishes linearly in $|\omega|$ as $\omega \to 0$. Consider now $\operatorname{Re}{}^0\Pi^{+-}_{AA}(\omega)$, in particular for $\omega = 0$. Using equation (2.22) together with the identity

$$\mathcal{G}_{A\uparrow}(\omega) - \mathcal{G}_{A\downarrow}(\omega) = -U|\mu|\mathcal{G}_{A\downarrow}(\omega)\mathcal{G}_{A\uparrow}(\omega) \tag{2.24}$$

(that follows from equation (2.12)), equation (2.18) yields

$$U\operatorname{Re}{}^0\Pi^{+-}_{AA}(\omega = 0) = \frac{1}{|\mu|}\int_{-\infty}^{0} d\omega\ [D^0_{A\uparrow}(\omega) - D^0_{A\downarrow}(\omega)]. \tag{2.25a}$$

For the flat-band case in particular, this is given explicitly by (cf. equations (2.15), (2.16))

$$U\operatorname{Re}{}^0\Pi^{+-}_{AA}(\omega = 0) = \frac{1}{|\tilde{\mu}|}\tan^{-1}(\tilde{U}|\tilde{\mu}|). \tag{2.25b}$$

2.2.2. Low-energy spin-flip scale. Since $\operatorname{Im}{}^0\Pi^{+-}_{AA}(\omega = 0) = 0$, the behaviour of $\Pi^{+-}_{AA}(\omega = 0)$ (equation (2.20)) is controlled by $\operatorname{Re}{}^0\Pi^{+-}_{AA}(\omega = 0)$. A number of important observations then follow directly from equation (2.25).

(i) Consider first *restricted* HF, where $|\mu| = 0$ is enforced for all U (the same results naturally hold for UHF when $|\mu| = 0$). From equation (2.25*b*) appropriate to the flat-band case, equation (2.20) yields

$$\pi\Delta_0\operatorname{Re}\Pi^{+-}_{AA}(\omega = 0) = [1 - \tilde{U}]^{-1} \qquad \text{RHF.} \tag{2.26}$$

For $\tilde{U} = U/\pi\Delta_0 > 1$—where UHF predicts an impurity local moment—equation (2.26) violates the positivity condition, equation (2.21*b*). This is well known (see e.g. [2]): it simply reflects the fact that the single-determinantal RHF mean-field state is unstable to particle–hole excitations—which is of course what is probed by the RPA Π [19]—and in that sense is thus physically unacceptable for $\tilde{U} > 1$.

(ii) This is in contrast to the mean-field UHF state with $|\mu| \neq 0$: it is not unstable to particle–hole excitations. At pure UHF level, quite generally, the local moment is determined *self-consistently* from equation (2.15) (or (2.16) for the specific flat-band case); which solution we denote from now on by $|\mu| = |\mu_0|$. From equation (2.25*a*) it follows directly that $U\,\mathrm{Re}\,{}^0\Pi^{+-}_{\mathrm{AA}}(\omega = 0) = 1$, and in consequence the transverse spin $\Pi^{+-}_{\mathrm{AA}}(\omega)$ has a pole at $\omega = 0$. While the mean-field state is stable, the $\omega = 0$ pole arises physically because the UHF ground state is a degenerate doublet, whence there is no energy cost to flip a spin. Physically, this behaviour is entirely correct for an *insulating* host—where the hybridization $\Delta_{\mathrm{I}}(\omega)$ has a gap in the vicinity of the Fermi level, $\omega = 0$. But it is clearly incorrect for the Fermi liquid ground state of the gapless Anderson model where the characteristic energy for spin-flip excitations is finite and of the order of the Kondo scale.

(iii) The latter behaviour is however *entirely specific to the UHF level of local moment self-consistency*: $U^0\Pi^{+-}_{\mathrm{AA}}(\omega = 0) = 1$ if and only if $|\mu| = |\mu_0|$, as follows from equation (2.25*a*). In the flat-band case, for example, it is readily shown explicitly from equation (2.25*b*) (see also below) that $U^0\Pi^{+-}_{\mathrm{AA}}(\omega = 0) < 1$ for any $|\mu| > |\mu_0|$. In describing single-particle spectra beyond pure UHF level, as in the following sections, this is the relevant case: the local moment $|\mu|$ will no longer be given by the UHF self-consistency equation (2.15), an $\omega = 0$ spin-flip pole will no longer arise, and $\mathrm{Im}\,\Pi^{+-}_{\mathrm{AA}}(\omega)$ will instead contain a resonance centred on some non-zero frequency, ω_{m}. As will be seen, this is in part the origin of the self-consistently determined Kondo scale within the present approach.

From the above we will clearly require, for *arbitrary* $|\mu|$, the ω-dependence of ${}^0\Pi^{+-}_{\alpha\alpha}(\omega)$ (and hence $\Pi^{+-}_{\alpha\alpha}$), technical details of which are now given. For the specific flat-band case, ${}^0\Pi^{+-}_{\alpha\alpha}(\omega)$ can be found analytically; the result is given in the appendix. To obtain the low-ω behaviour of $\Pi^{+-}_{\alpha\alpha}(\omega)$, and in particular the above-mentioned resonance, we perform a low-frequency expansion of ${}^0\Pi^{+-}_{\mathrm{AA}}(\omega) = \mathrm{Re}\,{}^0\Pi^{+-}_{\mathrm{AA}}(\omega) + \mathrm{i}\,\mathrm{Im}\,{}^0\Pi^{+-}_{\mathrm{AA}}(\omega)$ as follows, quite generally.

$$\Delta_0\,\mathrm{Im}\,{}^0\Pi^{+-}_{\mathrm{AA}}(\omega) = c|\tilde{\omega}| + \mathcal{O}(\tilde{\omega}^2) \tag{2.27}$$

where

$$\tilde{\omega} = \omega/\Delta_0 \tag{2.28}$$

is the reduced frequency; the coefficient c follows from equation (2.23*b*) (using equation (2.12*c*)), and is given generally by

$$c = \frac{1}{\pi(x^2+1)^2} \tag{2.29}$$

where (see also equation (2.16*b*))

$$x = \frac{\frac{1}{2}U|\mu|}{\Delta_0} = \tilde{U}|\tilde{\mu}|. \tag{2.30}$$

Similarly, defining

$$d(\omega) = \frac{1}{U} - \mathrm{Re}\,{}^0\Pi^{+-}_{\mathrm{AA}}(\omega) \tag{2.31a}$$

we expand

$$\Delta_0 d(\omega) = d_0 - d_1\tilde{\omega} + d_2\tilde{\omega}^2 + \mathcal{O}(\tilde{\omega}^3) \tag{2.31b}$$

where, from equation (2.25*a*),

$$d_0 = \frac{1}{\pi\tilde{U}}\left\{1 - \frac{1}{|\mu|}\int_{-\infty}^{0} \mathrm{d}\omega\ [D^0_{\mathrm{A}\uparrow}(\omega) - D^0_{\mathrm{A}\downarrow}(\omega)]\right\}. \tag{2.32a}$$

The coefficients d_i follow from the low-ω asymptotics of $\mathrm{Re}\,{}^0\Pi^{+-}_{\mathrm{AA}}(\omega)$, given explicitly in the appendix for the flat-band case, and for which

$$d_0 = \frac{1}{\pi\tilde{U}}\left\{1 - \frac{\tan^{-1}(\tilde{U}|\tilde{\mu}|)}{|\tilde{\mu}|}\right\} \tag{2.32b}$$

$$d_1 = \frac{1}{2\pi x}\left\{\frac{1}{x}\tan^{-1}(x) + \frac{(x^2-1)}{(x^2+1)^2}\right\} > 0. \tag{2.32c}$$

Equations (2.20) and (2.31) yield (generally)

$$\Delta_0\,\mathrm{Re}\,\Pi^{+-}_{\mathrm{AA}}(\omega=0) = \frac{(1-\pi\tilde{U}d_0)}{(\pi\tilde{U})^2 d_0} \tag{2.33a}$$

whence the stability condition equation (2.21*b*) is satisfied provided

$$0 \leqslant \pi\tilde{U}d_0 < 1. \tag{2.33b}$$

For the flat-band case, using equation (2.32*b*), this amounts simply to the above-mentioned condition that, for any chosen $\tilde{U}$, $|\tilde{\mu}| \geqslant |\tilde{\mu}_0|$ (with $|\tilde{\mu}_0| = \tan^{-1}(\tilde{U}|\tilde{\mu}_0|)$ the pure UHF local moment).

As mentioned above, $\mathrm{Im}\,\Pi^{+-}_{\mathrm{AA}}(\omega)$ contains in general a low-frequency resonance. To illustrate this at a simple (and in practice numerically very accurate) level, consider an ω-interval sufficiently close to $\omega \simeq 0$ that ${}^0\Pi^{+-}_{\mathrm{AA}}(\omega)$ itself is dominated by its low-ω behaviour. From equations (2.27), (2.31) and (2.20), the ω-dependence of $\mathrm{Im}\,\Pi^{+-}_{\mathrm{AA}}(\omega)$ is then given explicitly by

$$\Delta_0\,\mathrm{Im}\,\Pi^{+-}_{\mathrm{AA}}(\omega) \simeq \frac{A}{\tilde{\omega}_{\mathrm{m}}}\frac{|\omega'|}{1-2\alpha\omega'+\omega'^2} \tag{2.34a}$$

in terms of the scaled frequency

$$\omega' = \tilde{\omega}/\tilde{\omega}_{\mathrm{m}} \tag{2.34b}$$

where

$$\tilde{\omega}_{\mathrm{m}} = \frac{d_0}{\sqrt{c^2 + d_1^2 + 2d_0d_2}} \tag{2.34c}$$

and A and $\alpha \in (0,1)$ are likewise $\tilde{U}$-dependent coefficients given by

$$A = \frac{1}{(\pi\tilde{U})^2}\frac{c}{(c^2+d_1^2+2d_0d_2)} \tag{2.35a}$$

$$\alpha = \frac{d_1}{\sqrt{c^2+d_1^2+2d_0d_2}}. \tag{2.35b}$$

The resonant structure of $\mathrm{Im}\,\Pi^{+-}_{\mathrm{AA}}(\omega)$ is immediately apparent from equation (2.34*a*), whose maximum value occurs (for any $\alpha \in (0,1)$) at $\omega' = 1$: the resonance is thus centred on $\tilde{\omega} = \tilde{\omega}_{\mathrm{m}}$ given explicitly by equation (2.34*c*). For illustration, $\mathrm{Im}\,\Pi^{+-}_{\mathrm{AA}}(\omega)$ is shown in

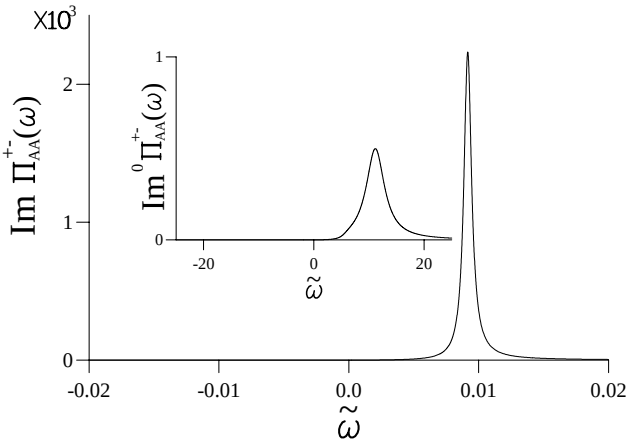

Figure 2. $\mathrm{Im}\,\Pi^{+-}_{\mathrm{AA}}(\omega)$ versus $\tilde{\omega} = \omega/\Delta_0$ for the flat-band case, with $\tilde{U} = U/\pi\Delta_0 = 4$ and $|\mu|/|\mu_0| = 1.001$, showing the low-ω spin-flip resonance. There are no further spectral features outside the range shown. Inset: the corresponding $\mathrm{Im}\,{}^0\Pi^{+-}_{\mathrm{AA}}(\omega)$, showing the high-energy Stoner band. Note the very different scales in the two figures.

figure 2 for the flat-band case with $\tilde{U} = 4$ and $|\mu|/|\mu_0| = 1.001$, and compared to the corresponding $\mathrm{Im}\,{}^0\Pi^{+-}_{\mathrm{AA}}(\omega)$ (equation (A.2)). The latter consists simply of a high-energy Stoner band centred (see (A.2)) on $\tilde{\omega} \sim U|\mu|/\Delta_0 = 2\tilde{U}|\tilde{\mu}| \sim 10^1$. For $\mathrm{Im}\,\Pi^{+-}_{\mathrm{AA}}(\omega)$ by contrast, it is seen that the vast majority of the spectral weight has been transferred to the low-ω resonance centred on the much smaller spin-flip scale $\tilde{\omega}_{\mathrm{m}} \sim 10^{-2}$, the intuitively obvious importance of which will be made explicit in the following sections where a specific criterion for self-consistently determining the local moment will be given.

3. Green functions

3.1. Two-self-energy description

In going beyond the simple mean-field approximation, single-particle processes must be coupled dynamically to the low-energy spin-flip excitations, as discussed in section 2.1. To this end the exact σ-spin impurity Green function is first expressed formally as

$$G(\omega) = \frac{1}{2}[G_{\mathrm{A}\sigma}(\omega) + G_{\mathrm{B}\sigma}(\omega)] \tag{3.1}$$

where

$$G_{\alpha\sigma}(\omega) = [\omega + \mathrm{i}\eta\,\mathrm{sgn}(\omega) - \Delta(\omega) - \tilde{\Sigma}_{\alpha\sigma}(\omega)]^{-1} \tag{3.2}$$

with ω-dependent interaction self-energies $\tilde{\Sigma}_{\alpha\sigma}(\omega)$. As at UHF level (equation (2.13)), up–down spin symmetry and particle–hole symmetry for the spectral densities $D_{\alpha\sigma}(\omega) = -\pi^{-1}\,\mathrm{sgn}(\omega)\,\mathrm{Im}\,G_{\alpha\sigma}(\omega)$ imply

$$D_{\mathrm{A}\sigma}(\omega) = D_{\mathrm{B}-\sigma}(\omega) \tag{3.3a}$$

$$= D_{\mathrm{A}-\sigma}(-\omega) \tag{3.3b}$$

respectively. For the associated Green functions $G_{\alpha\sigma}(\omega) = G^{+}_{\alpha\sigma}(\omega) + G^{-}_{\alpha\sigma}(\omega)$, a Hilbert transform of equations (3.3) yields directly

$$G^{\pm}_{\alpha\sigma}(\omega) = G^{\pm}_{\bar{\alpha}-\sigma}(\omega) \tag{3.4a}$$

$$= -G^{\mp}_{\alpha-\sigma}(-\omega) \tag{3.4b}$$

(where $\bar{\alpha} = \mathrm{B}$ or A for $\alpha = \mathrm{A}$ or B); from which, since $\Delta(\omega) = -\Delta(-\omega)$, it follows from equation (3.2) that

$$\tilde{\Sigma}_{\alpha\sigma}(\omega) = \tilde{\Sigma}_{\bar{\alpha}-\sigma}(\omega) \tag{3.5a}$$

$$= -\tilde{\Sigma}_{\bar{\alpha}\sigma}(-\omega). \tag{3.5b}$$

Likewise, equations (3.4) with (3.1) yield

$$G(\omega) = -G(-\omega) \tag{3.6a}$$

and show also that $G(\omega)$ is correctly independent of spin, σ; while equation (3.6*a*) itself correctly implies

$$\Sigma(\omega) = -\Sigma(-\omega) \tag{3.6b}$$

for the interaction self-energy defined by equation (2.7). Notice further from equations (3.1), (3.2) and (2.10) that a necessary/sufficient condition for the single-particle spectrum $D(\omega = 0)$ to be pinned at its non-interacting value (or equivalently for the Friedel sum rule to be satisfied) is

$$\tilde{\Sigma}_{\alpha\sigma}(\omega = 0) = 0. \tag{3.7}$$

Equations (3.3)–(3.6) merely express basic symmetries, which must of course be satisfied by any approximate theory. Equation (3.5) in particular shows that it is sufficient to consider only one of the $\tilde{\Sigma}_{\alpha\sigma}(\omega)$, say $\tilde{\Sigma}_{\mathrm{A}\uparrow}(\omega)$: the remainder follow from it by symmetry. $G(\omega)$ then follows from equations (3.1) and (3.2); direct comparison of which with equation (2.7) permits, if desired, $\Sigma(\omega)$ to be related to $\tilde{\Sigma}_{\mathrm{A}\uparrow}(\omega)$; specifically

$$\Sigma(\omega) = \frac{\frac{1}{2}\{\tilde{\Sigma}_{\mathrm{A}\uparrow}(\omega) - \tilde{\Sigma}_{\mathrm{A}\uparrow}(-\omega) + 2g(\omega)\tilde{\Sigma}_{\mathrm{A}\uparrow}(\omega)\tilde{\Sigma}_{\mathrm{A}\uparrow}(-\omega)\}}{1 - \frac{1}{2}g(\omega)[\tilde{\Sigma}_{\mathrm{A}\uparrow}(\omega) - \tilde{\Sigma}_{\mathrm{A}\uparrow}(-\omega)]} \tag{3.8}$$

where $g(\omega)$ is the non-interacting Green function, equation (2.4).

The $\tilde{\Sigma}_{\alpha\sigma}(\omega)$ are naturally not calculable exactly, but diagrammatic perturbation theory, expressed in terms of the bare propagators $\mathcal{G}_{\alpha\sigma}(\omega)$ (equation (2.12*a*)) and interaction U, can be employed to construct suitable approximations as described in section 3.2. In this regard it is helpful to separate the full interaction self-energies as

$$\tilde{\Sigma}_{\mathrm{A}\sigma}(\omega) = -\frac{\sigma}{2}U|\mu| + \Sigma_{\mathrm{A}\sigma}(\omega) \tag{3.9}$$

where the $\Sigma_{\alpha\sigma}(\omega)$—to which the symmetries equations (3.5) also apply—exclude the first-order ω-independent UHF-type contribution of $\pm U|\mu|/2$, and contain the dynamics on which we wish to focus. This we now consider.

3.2. Self-energy approximation

The basic approximation we consider for the self-energies $\Sigma_{\alpha\sigma}(\omega)$ is shown in figure 3(a), using the same diagrammatic notation as figure 1. It vanishes in the atomic limit and—considering the forward time direction for convenience—describes processes in which having added, say, a $\sigma = \uparrow$-spin electron to a $-\sigma = \downarrow$-spin occupied (B-type) impurity at $t = 0$, the $\downarrow$ spin already present hops off the site leaving behind it a spin flip, before returning again at a later time, t. All ladder interactions of the resultant particle–hole pair—reflecting the created spin flip—are included; their sum is exactly $U^2\Pi^{-+}_{ii}(\omega)$ $(=U^2\Pi^{+-}_{ii}(-\omega))$ as given by figure 1 and equation (2.20). The approximation is motivated on physical grounds: it captures the dynamical spin-flip scattering argued for physically in section 2.1, and known e.g. from Anderson's poor man's scaling [20] to be essential

(a)

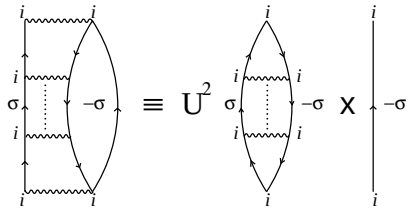

(b)

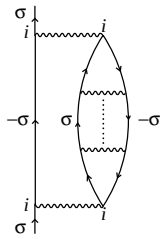

Figure 3. (a) The basic approximation to $\Sigma_{i\sigma}$ used in the present work, with the same notation as figure 1. (b) Equivalent recasting of (a), including ingoing and outgoing σ-spin propagators, to illustrate the spin-flip scattering involved.

in describing the Kondo limit; this is particularly clear from the equivalent recasting of $\Sigma_{\alpha\sigma}(\omega)$ shown in figure 3(b).

Explicitly, $\Sigma_{A\uparrow}(\omega)$ is given by

$$\Sigma_{A\uparrow}(\omega) = U^2 \int_{-\infty}^{\infty} \frac{d\omega_1}{2\pi i}\ \Pi^{+-}_{AA}(\omega_1)\mathcal{G}_{A\downarrow}(\omega_1+\omega). \tag{3.10}$$

Using the spectral representation for $\Pi^{+-}_{AA}(\omega)$, equation (2.21*a*), together with

$$\mathcal{G}^{\pm}_{\alpha\sigma}(\omega) = \int_{-\infty}^{\infty} \frac{d\omega_1}{2\pi i}\ \frac{\mathcal{G}_{\alpha\sigma}(\omega_1)}{\omega-\omega_1 \pm i\eta} \tag{3.11}$$

equation (3.10) reduces to

$$\Sigma_{A\uparrow}(\omega) = U^2 \int_{-\infty}^{\infty} \frac{d\omega_1}{\pi}\ \mathrm{Im}\,\Pi^{+-}_{AA}(\omega_1)\left[\theta(\omega_1)\mathcal{G}^{-}_{A\downarrow}(\omega_1+\omega) + \theta(-\omega_1)\mathcal{G}^{+}_{A\downarrow}(\omega_1+\omega)\right] \tag{3.12}$$

from which the low-frequency behaviour of $\mathrm{Im}\,\Sigma_{A\uparrow}(\omega)$ is now readily deduced. Since $\mathrm{Im}\,\mathcal{G}^{\pm}_{\alpha\sigma}(\omega) = \mp\pi D^0_{\alpha\sigma}(\omega)\theta(\pm\omega)$ (see equation (2.22)), equation (3.12) yields

$$\begin{aligned}\mathrm{Im}\,\Sigma_{A\uparrow}(\omega) = {} & \theta(-\omega)U^2 \int_0^{|\omega|} d\omega_1\ \mathrm{Im}\,\Pi^{+-}_{AA}(\omega_1) D^0_{A\downarrow}(\omega_1+\omega) \\ & -\theta(\omega)U^2 \int_{-|\omega|}^{0} d\omega_1\ \mathrm{Im}\,\Pi^{+-}_{AA}(\omega_1) D^0_{A\downarrow}(\omega_1+\omega)\end{aligned} \tag{3.13}$$

from which follow three important results.

(i) $\mathrm{Im}\,\Sigma_{A\uparrow}(\omega=0)=0$, i.e. vanishes at the Fermi level.

(ii) Since $\mathrm{Im}\,\Pi^{+-}_{\alpha\alpha}(\omega) \geqslant 0$ and $D^0_{\alpha\sigma}(\omega) \geqslant 0$ for all ω, $\mathrm{sgn}(\mathrm{Im}\,\Sigma_{A\uparrow}(\omega)) = -\mathrm{sgn}(\omega)$, whence $\Sigma_{A\uparrow}(\omega)$ is of the form

$$\Sigma_{A\uparrow}(\omega) = \Sigma^{R}_{A\uparrow}(\omega) - i\,\mathrm{sgn}(\omega)\Sigma^{I}_{A\uparrow}(\omega) \tag{3.14a}$$

with

$$\Sigma^{I}_{A\uparrow}(\omega) \geqslant 0. \tag{3.14b}$$

(iii) Since $\mathrm{Im}\,\Pi^{+-}_{AA}(\omega)$ vanishes linearly in $|\omega|$ as $\omega \to 0$ (see equations (2.23*b*), (2.20)),

$$\Sigma^{I}_{A\uparrow}(\omega) \propto \omega^2 \qquad \omega \to 0. \tag{3.15a}$$

Specifically, from equation (3.13),

$$\Sigma^{\mathrm{I}}_{\mathrm{A}\uparrow}(\omega) \overset{\omega\to 0}{\sim} \left(\frac{U^2}{2} D^0_{\mathrm{A}\downarrow}(0) \lim_{\omega\to 0}\left(\frac{\operatorname{Im}\Pi^{+-}_{\mathrm{AA}}(\omega)}{|\omega|}\right)\right)\omega^2 \tag{3.15b}$$

$$= \frac{U^2}{2} D^0_{\mathrm{A}\downarrow}(0) A \left[\frac{\omega}{\omega_{\mathrm{m}}}\right]^2 \tag{3.15c}$$

where equation (3.15*c*) follows from equation (2.34*a*) (which, given Π^{+-}_{AA} in RPA form, is asymptotically exact as $\omega \to 0$).

For the single-particle spectrum to be pinned at the Fermi level, $\tilde{\Sigma}_{\alpha\sigma}(\omega = 0) = 0$ is required (equation (3.7)); and since $\operatorname{Im}\tilde{\Sigma}_{\alpha\sigma}(\omega) = \operatorname{Im}\Sigma_{\alpha\sigma}(\omega)$ (see equation (3.9)), $\operatorname{Im}\tilde{\Sigma}_{\alpha\sigma}(\omega = 0) = 0$ automatically. From equation (3.9), the requirement that $\operatorname{Re}\tilde{\Sigma}_{\alpha\sigma}(\omega = 0) = 0$ is

$$\Sigma^{\mathrm{R}}_{\mathrm{A}\uparrow}(\omega = 0) = \frac{1}{2} U|\mu|. \tag{3.16}$$

It is this equation that we use to determine the local moment $|\mu|$: $\Sigma^{\mathrm{R}}_{\mathrm{A}\uparrow}(\omega)$, given explicitly from equation (3.12), is itself a function of $|\mu|$ via the dependence of Π^{+-}_{AA} and $\mathcal{G}^{\pm}_{\mathrm{A}\downarrow}$ thereon, whence equation (3.16) is a self-consistency equation for $|\mu|$. The local moment is thus self-consistently determined by enforcing the $\omega = 0$ pinning of the single-particle spectrum, or equivalently the Friedel sum rule. We add that there is ample precedent for enforcing the Friedel sum rule: it is for example employed in phenomenological Fermi liquid theory (see e.g. [2, 21]) and, for the asymmetric Anderson model in particular, in studies using conventional finite-order perturbation theory in U about the non-interacting limit [16]. And its consequences are far reaching, particularly in the strong-coupling regime of central interest, as will be seen in the following sections.

Before proceeding we comment briefly on the functional form of the self-consistency equation (3.16), with $\Sigma_{\mathrm{A}\uparrow}(\omega)$ given by equation (3.12). The bare propagators $\mathcal{G}_{\alpha\sigma}$ (equation (2.12)), and hence ${}^0\Pi^{+-}_{\mathrm{AA}}$ (equation (2.18)), depend on U and $|\mu|$ solely via the combination $\frac{1}{2}U|\mu|$. Thus, defining $x = \frac{1}{2}U|\mu|/\Delta_0$, equation (3.16) is of the form

$$f(U; x) = x \qquad x = \frac{1}{2} U|\mu|/\Delta_0 \tag{3.17}$$

where the explicit U-dependence of $f(U; x) = \Delta_0^{-1}\Sigma^{\mathrm{R}}_{\mathrm{A}\uparrow}(\omega = 0)$ stems simply from the dependence of $\Pi^{+-}_{\mathrm{AA}} = {}^0\Pi^{+-}_{\mathrm{AA}}/(1 - U\,{}^0\Pi^{+-}_{\mathrm{AA}})$ on U itself, and from the prefactor U^2 in equation (3.12). Equation (3.17) is most efficiently solved either for x, given U, or for U, given x; $|\mu|$ is thereby obtained self-consistently as a function of U.

4. Strong-coupling asymptotics

The procedure for determining the impurity Green function is simply summarized: $G(\omega)$ is given by equations (3.1), (3.2), with interaction self-energy $\tilde{\Sigma}_{\mathrm{A}\uparrow}(\omega) = -\frac{1}{2}U|\mu| + \Sigma_{\mathrm{A}\uparrow}(\omega)$ (equation (3.9)), and $\Sigma_{\mathrm{A}\uparrow}(\omega)$ given explicitly by equation (3.12); the remaining $\tilde{\Sigma}_{\alpha\sigma}$s follow by symmetry, equation (3.5), specifically $\tilde{\Sigma}_{\mathrm{B}\uparrow}(\omega) = -\tilde{\Sigma}_{\mathrm{A}\uparrow}(-\omega)$; and the local moment is determined self-consistently from equation (3.16). This permits a straightforward determination of the single-particle spectrum for an arbitrary symmetric hybridization function satisfying equation (2.6); resultant spectra for the particular flat-band case will be shown in section 5.

In this section we seek first to establish the $U \to \infty$ strong-coupling asymptotics. We consider separately (i) the spectral asymptotics at low energies, in particular the origin

and U-dependence of the Kondo scale, the emergence of Fermi liquid behaviour and the quasiparticle form (equation (2.9*a*)) for $G(\omega)$; and, relatedly, (ii) the asymptotic behaviour of the high-energy Hubbard satellites.

4.1. Low energies

4.1.1. Kondo scale. The low-frequency behaviour of $\operatorname{Im}\Sigma_{A\uparrow}(\omega)$ has been established in the previous section, equations (3.13)–(3.15). We now consider the low-ω behaviour of $\Sigma^{R}_{A\uparrow}(\omega)$, beginning with $\Sigma^{R}_{A\uparrow}(\omega=0)$ given explicitly from equation (3.12) by

$$\Sigma^{R}_{A\uparrow}(\omega=0) = U^2 \int_{-\infty}^{\infty} \frac{d\omega_1}{\pi}\, \operatorname{Im}\Pi^{+-}_{AA}(\omega_1)\left[\theta(\omega_1)\operatorname{Re}\mathcal{G}^{-}_{A\downarrow}(\omega_1) + \theta(-\omega_1)\operatorname{Re}\mathcal{G}^{+}_{A\downarrow}(\omega_1)\right]. \tag{4.1}$$

$\operatorname{Im}\Pi^{+-}_{AA}(\omega)$ has been illustrated in figure 2, and the $U\to\infty$ asymptotic form of $\Sigma^{R}_{A\uparrow}(0)$ is readily deduced from two properties of $\operatorname{Im}\Pi^{+-}_{AA}(\omega)$.

(i) First, as $U\to\infty$, the spectral weight of $\operatorname{Im}\Pi^{+-}_{AA}(\omega)$ is confined entirely to frequencies $\omega>0$; specifically, one finds

$$\int_{0}^{\infty} \frac{d\omega}{\pi}\, \operatorname{Im}\Pi^{+-}_{AA}(\omega) \overset{U\to\infty}{\sim} 1 \tag{4.2}$$

which behaviour reflects physically the saturation of the local moment in strong coupling; the corrections to equation (4.2) are at least $\mathcal{O}(U^{-1})$ (and precisely $\mathcal{O}(U^{-1})$ for the flat-band case). By contrast, the integrated spectral weight of $\operatorname{Im}\Pi^{+-}_{AA}(\omega)$ for frequencies $\omega<0$ is found to be at least $\mathcal{O}(U^{-1})$. In consequence, the second term on the right-hand side of equation (4.1) may be neglected in determining the strong-coupling asymptotics of $\Sigma^{R}_{A\uparrow}(0)$.

(ii) As illustrated in figure 2, the resonance in $\operatorname{Im}\Pi^{+-}_{AA}(\omega)$ occurs on a low-energy spin-flip scale, ω_m, that is found to diminish rapidly with increasing U (and whose explicit U-dependence we establish below). $\operatorname{Im}\Pi^{+-}_{AA}(\omega)$ is thus effectively non-zero only on the scale of ω_m; and on scales of this order, $\mathcal{G}^{-}_{A\downarrow}(\omega)$ is a slowly varying function of frequency. Equation (4.1) thus reduces asymptotically to

$$\begin{aligned}\Sigma^{R}_{A\uparrow}(\omega=0) &\overset{U\to\infty}{\sim} U^2 \operatorname{Re}\mathcal{G}^{-}_{A\downarrow}(\omega_m)\int_{0}^{\infty}\frac{d\omega_1}{\pi}\,\operatorname{Im}\Pi^{+-}_{AA}(\omega_1)\\ &= U^2\operatorname{Re}\mathcal{G}^{-}_{A\downarrow}(\omega_m).\end{aligned} \tag{4.3}$$

Consider now the low-ω behaviour of $\operatorname{Re}\mathcal{G}^{-}_{A\downarrow}(\omega)$ itself, given by

$$\operatorname{Re}\mathcal{G}^{-}_{A\downarrow}(\omega) = \int_{-\infty}^{0} d\omega_1\, D^{0}_{A\downarrow}(\omega_1)\,\mathrm{P}\left(\frac{1}{\omega-\omega_1}\right) \tag{4.4}$$

as a one-side Hilbert transform of the spectral density $D^{0}_{A\downarrow}(\omega)$ (equation (2.12*c*)). The $\omega\to0$ behaviour of $\operatorname{Re}\mathcal{G}^{-}_{A\downarrow}(\omega)$ is dominated by the logarithmic singularity arising necessarily because $D^{0}_{A\downarrow}(\omega=0)$ is non-vanishing. This asymptotic behaviour is captured by

$$\operatorname{Re}\mathcal{G}^{-}_{A\downarrow}(\omega) \overset{\omega\to0}{\sim} D^{0}_{A\downarrow}(0)\int_{-U}^{0} d\omega_1\,\mathrm{P}\left(\frac{1}{\omega-\omega_1}\right) \tag{4.5a}$$

$$= D^{0}_{A\downarrow}(0)\ln\left(\frac{U}{|\omega|}\right) \tag{4.5b}$$

where we have introduced a high-energy cut-off of order U. The latter is appropriate in the limit that the host bandwidth $D\to\infty$; for finite D, a cut-off of order $\min(D,U)$ is

instead appropriate. The specific cut-off used is inessential to the following arguments: the important point is that, as $\omega \to 0$, the prefactor to the log divergence is precisely $D^0_{A\downarrow}(0)$, itself given in general from equation (2.12*c*) by

$$D^0_{A\downarrow}(0) = \frac{\Delta_0 \pi^{-1}}{(\frac{1}{2}U|\mu|)^2 + \Delta_0^2} \tag{4.6}$$

(where $\Delta_R(\omega = 0) = 0$ from equation (2.6*a*), and $\Delta_0 = \Delta_I(\omega = 0)$). This is confirmed by explicit calculation of $\mathrm{Re}\,\mathcal{G}^-_{A\downarrow}(\omega)$ for the particular flat-band case, which gives

$$\mathrm{Re}\,\mathcal{G}^-_{A\downarrow}(\omega) = D^0_{A\downarrow}(\omega)\left\{\ln\left[\frac{[x^2+1]^{1/2}}{|\tilde{\omega}|}\right] + (\tilde{\omega} - x)\left[\frac{\pi}{2} - \tan^{-1}(x)\right]\right\} \tag{4.7}$$

where $\tilde{\omega} = \omega/\Delta_0$ and $x = \frac{1}{2}U|\mu|/\Delta_0$.

In strong coupling $U \to \infty$ ($|\mu| \to 1$), equation (4.6) gives quite generally

$$D^0_{A\downarrow}(0) \overset{U\to\infty}{\sim} \frac{1}{U^2}\frac{4\Delta_0}{\pi} \tag{4.8a}$$

$$= \frac{1}{U^2}\frac{4}{\pi^2 D(0)} \tag{4.8b}$$

where $D(0) = (\pi\Delta_0)^{-1}$ is the Fermi level spectral density (equation (2.10)); whence from equations (4.3), (4.5),

$$\Sigma^R_{A\uparrow}(\omega = 0) \overset{U\to\infty}{\sim} \frac{4}{\pi^2 D(0)} \ln\left(\frac{U}{\omega_m}\right). \tag{4.9}$$

The U-dependence of ω_m now follows immediately from the condition, equation (3.16), that the single-particle spectrum be pinned at the Fermi level, namely

$$\Sigma^R_{A\uparrow}(\omega = 0) \overset{U\to\infty}{\sim} \frac{U}{2}. \tag{4.10}$$

Equations (4.9), (4.10) yield

$$\omega_m \overset{U\to\infty}{\sim} U \exp\left(\frac{-\pi^2}{8} D(0) U\right) \tag{4.11a}$$

$$= U \exp\left(\frac{-\pi U}{8\Delta_0}\right). \tag{4.11b}$$

This is the Kondo scale, exponentially small in strong coupling. While the prefactor to the exponential, of order U (or $\min(D, U)$), merely reflects the cut-off used in equation (4.5*a*), the exponent itself is linear in U, with coefficient $-\pi/8\Delta_0$. This agrees precisely with the Bethe *ansatz* result [3] for the flat-band case (although equation (4.11) itself is not restricted to that case).

The above result for the Kondo scale has been obtained by simple, rather general arguments. We have further confirmed it both by direct numerical calculation (see also section 5) and, for the flat-band case, analytically: equation (2.34) for $\mathrm{Im}\,\Pi^{+-}_{AA}(\omega)$ may be used in equation (4.1) to determine $\Sigma^R_{A\uparrow}(0)$ explicitly; equation (4.11) again results for ω_m, given by equation (2.34*c*) and corresponding to the maximum in the resonance of $\mathrm{Im}\,\Pi^{+-}_{AA}(\omega)$. The latter may in turn be used to deduce how the self-consistent local moment $|\mu|$ approaches its strong-coupling asymptote of unity, and this we consider briefly.

$\tilde{\omega}_m = \omega_m/\Delta_0$ is given by equation (2.34*c*), and in strong coupling the coefficient $c \sim U^{-4}$ (see equation (2.29)), while

$$d_1 \overset{U\to\infty}{\sim} (\pi\tilde{U})^{-2} = (\Delta_0/U)^2. \tag{4.12}$$

(For the flat-band case this follows directly from equation (2.32*c*) ($x = \frac{1}{2}U|\mu|/\Delta_0 \overset{U\to\infty}{\sim} U/2\Delta_0$); and it is readily shown to be true in general.) From equation (2.34*c*), since $\tilde{\omega}_\mathrm{m}$ is exponentially small in strong coupling, so too is d_0; hence

$$\tilde{\omega}_\mathrm{m} \overset{U\to\infty}{\sim} \frac{d_0}{d_1} = (\pi\tilde{U})^2 d_0. \tag{4.13}$$

d_0 is given explicitly by equation (2.32), so for the flat-band case in particular (equation (2.32*b*))

$$\frac{\omega_\mathrm{m}}{U} \overset{U\to\infty}{\sim} \left(1 - \frac{\tan^{-1}(\tilde{U}|\tilde{\mu}|)}{|\tilde{\mu}|}\right). \tag{4.14a}$$

This is now solved for $|\tilde{\mu}| = (\pi/2)|\mu|$ and, since ω_m is exponentially small in strong coupling, gives

$$|\mu| \overset{U\to\infty}{\sim} |\mu_0| + \frac{\omega_\mathrm{m}}{U} \tag{4.14b}$$

where $|\mu_0|$ is the pure UHF local moment given via $|\tilde{\mu}_0| = \tan^{-1}(\tilde{U}|\tilde{\mu}_0|)$ and such that $|\mu_0| = 1 - (4\Delta_0/\pi U) + \mathcal{O}(U^{-2})$. With ω_m from equation (4.11), equation (4.14*b*) gives explicitly the U-dependence of the local moment $|\mu|$ determined self-consistently from the requirement, equation (3.16), that the single-particle spectrum is pinned at the Fermi level, $\omega = 0$.

4.1.2. Quasiparticle form. Having established the asymptotics of $\Sigma^\mathrm{R}_{\mathrm{A}\uparrow}(\omega)$ at $\omega = 0$, we consider now its leading low-ω behaviour. This may be determined from equation (3.12), by differentiating once with respect to ω under the integral using the asymptotic form equation (4.5*b*) for $\mathrm{Re}\,\mathcal{G}^-_{\mathrm{A}\downarrow}(\omega_1+\omega)$ (and neglecting the second term on the right-hand side of equation (3.12), for the same reason as in the asymptotic analysis of $\Sigma^\mathrm{R}_{\mathrm{A}\uparrow}(\omega = 0)$, equation (4.1) ff). This yields

$$\Sigma^\mathrm{R}_{\mathrm{A}\uparrow}(\omega) - \Sigma^\mathrm{R}_{\mathrm{A}\uparrow}(0) \overset{\substack{U\to\infty\\ \omega\to 0}}{\sim} -\omega\frac{4}{\pi^2 D(0)}\int_0^\infty \frac{\mathrm{d}\omega_1}{\pi}\,\frac{\mathrm{Im}\,\Pi^{+-}_{\mathrm{AA}}(\omega_1)}{|\omega_1|} \tag{4.15}$$

where equation (4.8) is used for $U^2 D_{\mathrm{A}\downarrow}(0)$. The lower integration limit may be extended with impunity to $\omega_1 = -\infty$ as $U \to \infty$: the relative correction is $\mathcal{O}(U^{-2})$ (as may be verified either numerically or by use of equation (2.34*a*)). Thus, using equation (2.21*b*),

$$\Sigma^\mathrm{R}_{\mathrm{A}\uparrow}(\omega) - \Sigma^\mathrm{R}_{\mathrm{A}\uparrow}(0) \overset{\substack{U\to\infty\\ \omega\to 0}}{\sim} -\omega\frac{4}{\pi^2 D(0)}\,\mathrm{Re}\,\Pi^{+-}_{\mathrm{AA}}(\omega = 0). \tag{4.16}$$

$\mathrm{Re}\,\Pi^{+-}_{\mathrm{AA}}(0)$ is given explicitly by equation (2.33*a*) which, using equation (4.13) and the fact that d_0 is itself exponentially small in strong coupling, reduces to $\mathrm{Re}\,\Pi^{+-}_{\mathrm{AA}}(0) \overset{U\to\infty}{\sim} 1/\omega_\mathrm{m}$. Hence the desired result

$$\tilde{\Sigma}^\mathrm{R}_{\mathrm{A}\uparrow}(\omega) = \Sigma^\mathrm{R}_{\mathrm{A}\uparrow}(\omega) - \Sigma^\mathrm{R}_{\mathrm{A}\uparrow}(0) \tag{4.17}$$

$$\overset{\substack{U\to\infty\\ \omega\to 0}}{\sim} -\frac{4}{\pi^2 D(0)}\frac{\omega}{\omega_\mathrm{m}} \tag{4.18a}$$

$$= -\frac{4\Delta_0}{\pi}\frac{\omega}{\omega_\mathrm{m}} \tag{4.18b}$$

(where equation (4.17) follows trivially from equations (3.9), (3.16)); we have also confirmed this numerically. Two further points should be noted.

(a) The leading low-ω corrections to equation (4.18) are $\mathcal{O}(\omega^2 \ln|\omega|)$ and $\mathcal{O}(\omega^2)$, the existence of which may be shown to follow on general grounds from equation (3.12) for $\Sigma^{\mathrm{R}}_{\mathrm{A}\uparrow}(\omega)$, due to the necessary logarithmic singularity in $\mathrm{Re}\,\mathcal{G}^{-}_{\mathrm{A}\downarrow}$ and the fact that $\mathrm{Im}\,\Pi^{+-}_{\mathrm{AA}}(\omega)/\omega$ is finite as $\omega \to 0$.

(b) Although the explicit coefficient of ω in equation (4.18) is naturally applicable only in strong coupling, the linearity of the self-energy, namely $\tilde{\Sigma}^{\mathrm{R}}_{\mathrm{A}\uparrow}(\omega) \propto \omega$ as $\omega \to 0$, is itself quite general as follows from a low-ω expansion of equation (3.12).

The above results, together with equation (3.15) for the imaginary part of the self-energy $\tilde{\Sigma}^{\mathrm{I}}_{\mathrm{A}\uparrow}(\omega)$ ($=\Sigma^{\mathrm{I}}_{\mathrm{A}\uparrow}(\omega)$ from equations (3.9), (3.14*a*)), lead directly to the low-frequency behaviour of the impurity Green function $G(\omega)$. Since $\tilde{\Sigma}^{\mathrm{R}}_{\mathrm{A}\uparrow}(\omega) \propto \omega$ and $\tilde{\Sigma}^{\mathrm{I}}_{\mathrm{A}\uparrow}(\omega) \propto \omega^2$ as $\omega \to 0$, the symmetries, equation (3.5), yield

$$\tilde{\Sigma}_{\mathrm{A}\sigma}(\omega) = \tilde{\Sigma}_{\mathrm{B}\sigma}(\omega) \qquad \omega \to 0 \tag{4.19a}$$

Hence, from equations (3.1), (3.2) for $G(\omega)$, together with the definition, equation (2.7), of the self-energy $\Sigma(\omega)$,

$$\tilde{\Sigma}_{\alpha\sigma}(\omega) = \Sigma(\omega) \qquad \omega \to 0 \tag{4.19b}$$

(for any σ or $\alpha = \mathrm{A}$, B): the low-frequency asymptotics of $\tilde{\Sigma}_{\mathrm{A}\uparrow}(\omega)$ are thus also those for $\Sigma(\omega)$; equations (3.14), (3.15*a*) in particular reduce to well known exact Fermi liquid results for $\Sigma(\omega)$ [22]. From equations (4.19*b*) and (2.7) it follows immediately that the low-ω behaviour of $G(\omega)$ takes correctly the quasiparticle form equation (2.9), namely

$$G(\omega) = \frac{1}{\omega/Z + \mathrm{i}\,\mathrm{sgn}(\omega)(\Delta_0 + \mathcal{O}(\omega^2))} \tag{4.20}$$

(to which we note only the real part of Σ contributes), the frequency scale of which is set by $\Delta_0 Z$. And from equation (4.18*b*) the quasiparticle weight in the strong-coupling (Kondo) limit is proportional to ω_{m},

$$\Delta_0 Z \overset{U\to\infty}{\sim} \frac{\pi}{4}\omega_{\mathrm{m}} \tag{4.21}$$

in terms of which the low-ω behaviour of $G(\omega)$ thus scales.

The significance of the Kondo scale within the present approach is further apparent from the preceding results. Equation (4.19*a*) shows that on the lowest frequency scales—or longest timescales—the interaction self-energies $\tilde{\Sigma}_{\alpha\sigma}(\omega)$ coincide, or equivalently, $G_{\mathrm{A}\sigma}(\omega) = G_{\mathrm{B}\sigma}(\omega)$. This reflects physically the restoration at sufficiently long times of the locally broken symmetry inherent in the zeroth-order mean-field (UHF) level of description, the characteristic timescale for symmetry restoration being the 'Kondo spin-flip time' $1/\omega_{\mathrm{m}}$ in strong coupling (alternatively, ω_{m} itself may be thought of as the rate of interconversion between the two local moment states A and B).

4.2. High energies

We consider now the strong-coupling asymptotics of the high-energy Hubbard satellites, centred on $\omega \sim \pm U/2$. In particular we show that the additional many-body broadening therein, argued for on simple physical grounds in section 2.1, emerges straightforwardly within the present approach.

Consider again equation (3.12) for the self-energy $\Sigma_{\mathrm{A}\uparrow}(\omega)$, and recall from section 4.1.1 that the spectral density $\mathrm{Im}\,\Pi^{+-}_{\mathrm{AA}}(\omega_1)$ occurs on frequency scales of order ω_{m}. Hence, for

frequencies $|\omega| \gg \omega_{\rm m}$,

$$U^{-2}\Sigma_{\rm A\uparrow}(\omega) \overset{|\omega|\gg\omega_{\rm m}}{\sim} \mathcal{G}^{-}_{\rm A\downarrow}(\omega)\int_0^\infty \frac{{\rm d}\omega_1}{\pi}\,{\rm Im}\,\Pi^{+-}_{\rm AA}(\omega_1) + \mathcal{G}^{+}_{\rm A\downarrow}(\omega)\int_{-\infty}^0 \frac{{\rm d}\omega_1}{\pi}\,{\rm Im}\,\Pi^{+-}_{\rm AA}(\omega_1). \tag{4.22}$$

To see the origin of the additional spectral broadening we focus on the imaginary part of the self-energy, ${\rm Im}\,\Sigma_{\rm A\uparrow}(\omega) = -{\rm sgn}(\omega)\Sigma^{\rm I}_{\rm A\uparrow}(\omega)$ (see equation (3.14*a*)); and consider for convenience the lower Hubbard band (LHB), $\omega < 0$. Since ${\rm Im}\,\mathcal{G}^{\pm}_{\rm A\downarrow}(\omega) = -{\rm sgn}(\omega)\pi D^0_{\rm A\downarrow}(\omega)\theta(\pm\omega)$ (from equation (2.22), the second term in equation (4.22) does not contribute for $\omega < 0$. Hence

$$\Sigma^{\rm I}_{\rm A\uparrow}(\omega) = \pi U^2 D^0_{\rm A\downarrow}(\omega)\int_0^\infty \frac{{\rm d}\omega_1}{\pi}\,{\rm Im}\,\Pi^{+-}_{\rm AA}(\omega_1) \tag{4.23a}$$

$$\overset{U\to\infty}{\sim} \pi U^2 D^0_{\rm A\downarrow}(\omega) \tag{4.23b}$$

where equation (4.2) is used. $D^0_{\rm A\downarrow}(\omega)$ is itself given by equation (2.12*c*) from which, in strong coupling and for frequencies $\omega \sim -U/2$, equation (4.23*b*) yields

$$\Sigma^{\rm I}_{\rm A\uparrow}(\omega) \overset{U\to\infty}{\sim} \Delta_{\rm I}(\omega) \qquad \omega \sim -\frac{U}{2}. \tag{4.24}$$

At frequencies $\omega \sim -U/2$ in the LHB, the impurity Green function itself is given explicitly as $U \to \infty$ by $G(\omega) \sim \frac{1}{2}G_{\rm A\uparrow}(\omega)$ (as follows from equation (3.1) noting that $D_{\rm B\uparrow}(\omega) = D_{\rm A\downarrow}(\omega)$ is centred on $\omega \sim +U/2$); and $G_{\rm A\uparrow}(\omega)$ follows from equation (3.2) with interaction self-energy $\tilde{\Sigma}_{\rm A\uparrow}(\omega) \overset{U\to\infty}{\sim} -\frac{1}{2}U + \Sigma_{\rm A\uparrow}(\omega)$ (see equation (3.9)). Thus, using equation (4.24),

$$G(\omega) \overset{U\to\infty}{\sim} \frac{\frac{1}{2}}{(\omega + \frac{1}{2}U) - 2{\rm i}\Delta_{\rm I}(\omega)} \qquad \omega \sim -\frac{U}{2} \tag{4.25}$$

where we have neglected $\Delta_{\rm R}(\omega)$ and $\Sigma^{\rm R}_{\rm A\uparrow}(\omega)$ (see below); the corresponding strong-coupling expression for $G(\omega)$ in the upper Hubbard band at frequencies $\omega \sim +U/2$ follows trivially from equation (4.25) via the symmetry $G(\omega) = -G(-\omega)$, and yields precisely equation (2.17*b*) for the flat-band case.

The present theory thus captures simultaneously the low-ω Kondo resonance, and the additional many-body broadening of the Hubbard bands reflected in the doubling of the satellite widths ($2\Delta_{\rm I}(\omega)$).

Finally, we comment briefly on the contribution of $\Sigma^{\rm R}_{\rm A\uparrow}(\omega)$ to the Hubbard satellites. We have neglected it in arriving at equation (4.25) above since it naturally makes no contribution to the width of the satellites and, as now clarified, gives *at most* an $\mathcal{O}(1)$ shift in their positions (i.e. $\omega \sim \pm(U/2)(1 + \mathcal{O}(1/U))$). To calculate $\Sigma^{\rm R}_{\rm A\uparrow}(\omega \sim -U/2)$ the second term on the right-hand side of equation (4.22) must be considered explicitly. This can be done analytically and, for the flat-band case, leads to $\tilde{\Sigma}^{\rm R}_{\rm A\uparrow}(\omega \sim -U/2) \sim -(U/2)(1+4\Delta_0/\pi U)$; the Hubbard bands are thus centred on $\omega \sim \mp(U/2)(1+4\Delta_0/\pi U)$ in strong coupling. This behaviour is however specific to the flat-band problem (with bandwidth $D \to \infty$): for any other case it may be shown that the leading corrections to the position of the Hubbard satellites are $\mathcal{O}(1/U)$, i.e. they are centred on $\omega \sim \pm(U/2)(1 + \mathcal{O}(U^{-2}))$.

5. Results

The general procedure used to obtain the impurity Green function has been summarized in section 4. For tangibility we consider now the flat-band case. Figure 4 shows the resultant

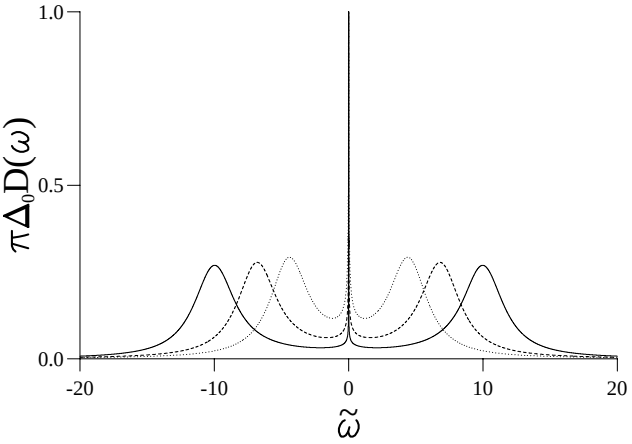

Figure 4. $\pi\Delta_0 D(\omega)$ versus $\tilde{\omega} = \omega/\Delta_0$ for the flat-band case with $\tilde{U} = 6$ (solid line), 4 (dashed line) and 2.5 (dotted line).

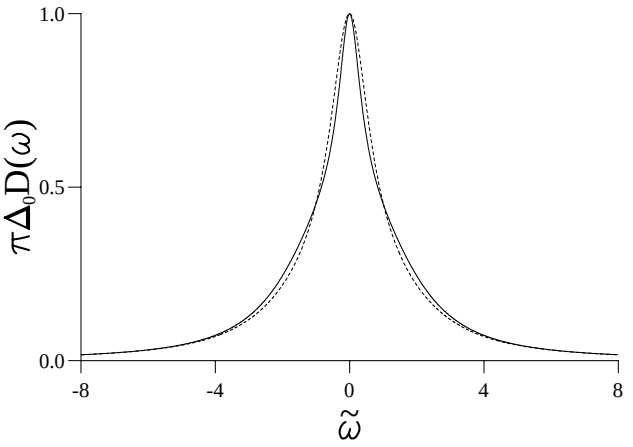

Figure 5. $\pi\Delta_0 D(\omega)$ versus $\tilde{\omega} = \omega/\Delta_0$ for the flat-band case with $\tilde{U} = 0.6$ (solid line), compared to the result from straight second-order perturbation theory in U about the non-interacting limit (dashed line).

single-particle spectrum, $\pi\Delta_0 D(\omega)$ versus $\tilde{\omega}$ $(=\omega/\Delta_0)$, for $\tilde{U}$ $(=U/\pi\Delta_0) = 6$, 4 and 2.5. $D(\omega)$ is correctly normalized to unity; and the spectrum is of course pinned at the Fermi level itself, such that $\pi\Delta_0 D(0) = 1$. The two expected spectral features are evident: a many-body Kondo resonance whose width diminishes rapidly with increasing $\tilde{U}$, and the Hubbard satellites which correspondingly shift to progressively higher frequencies. Before proceeding we also add that, while naturally designed to capture strong-coupling behaviour, the present theory is nonetheless well behaved with decreasing $\tilde{U}$, and evolves smoothly to the non-interacting limit. For illustration figure 5 shows the impurity spectrum for $\tilde{U} = 0.6$, compared to the result from straight second-order perturbation theory in U about the non-interacting limit, from which it differs only slightly and to which it reduces precisely to (and including) $\mathcal{O}(U^2)$ as $U \to 0$.

The approach to strong-coupling behaviour is seen clearly in the $\tilde{U}$-dependence of $\tilde{\omega}_K = \omega_K/\Delta_0$, defined as the half-width at half-maximum of $D(\omega)$ (and reducing to the

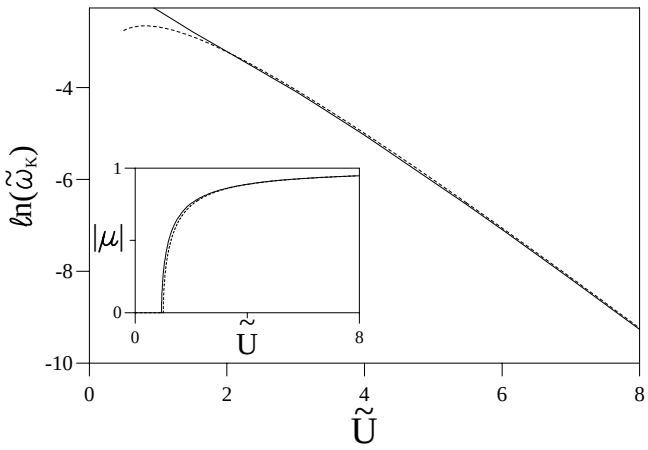

Figure 6. Strong-coupling behaviour of the Kondo scale: $\ln\tilde{\omega}_K$ versus $\tilde{U}$ for the flat-band case (solid line), compared to the asymptotic form $\tilde{\omega}_K = \beta\tilde{U}\exp(-\pi^2\tilde{U}/8)$ with $\beta = 0.24$ (dashed line). Inset: self-consistent local moment $|\mu|$ versus $\tilde{U}$ (solid line), contrasted with its UHF counterpart $|\mu_0|$ (dashed line).

Kondo scale in strong coupling where $\omega_K \propto \omega_m$). Figure 6 shows $\ln\tilde{\omega}_K$ versus $\tilde{U}$, and confirms the analytic result of the preceding sections: the strong-coupling asymptote is found to be $\tilde{\omega}_K \sim \beta\tilde{U}\exp(-\pi^2\tilde{U}/8)$ in agreement with equation (4.11), with the constant $\beta = 0.24$ determined numerically. The inset to figure 6 shows also the $\tilde{U}$-dependence of the self-consistent local moment $|\mu|$, compared to its UHF counterpart $|\mu_0|$. For $\tilde{U} < \tilde{U}_0$, $|\mu| = 0$ and $\mathrm{Re}\,\Pi^{+-}_{AA}(\omega = 0) \propto [1 - \tilde{U}]^{-1}$ is thus given by equation (2.26). The self-consistent determination of $|\mu|$ is however seen to reduce $\tilde{U}_0$ to $\sim$0.94 from $\tilde{U}_0 = 1$ at mean-field level, whence $\tilde{U} = \tilde{U}_0$ no longer corresponds to an instability: $\mathrm{Re}\,\Pi^{+-}_{AA}(0)$ evolves smoothly as $\tilde{U}$ passes through $\tilde{U}_0$, and is both positive definite and finite for all $\tilde{U}$. For $\tilde{U} > \tilde{U}_0$, $|\mu|$ increases strongly and rapidly becomes exponentially close to $|\mu_0|$ (as argued in section 4.1; see equation (4.14*b*)). In fact, from the behaviour of both $\tilde{\omega}_K$ and $|\mu|$, strong-coupling behaviour sets in over a narrow $\tilde{U}$-interval above $\tilde{U}_0$, and is in practice established by $\tilde{U} \sim 2$ or so. This concurs with weak-coupling studies based on low-order perturbation theory in U, which likewise identify the onset of strong-coupling behaviour at $\tilde{U} \sim 2$; see e.g. [16]. Quantitatively, however, the present calculations probably predict the persistence of essentially strong-coupling behaviour down to somewhat too low values of $\tilde{U}$. This is for example hinted at by the $\tilde{U} = 2.5$ spectrum in figure 4, and is hardly surprising since the theory seeks to capture the strong-coupling asymptotics; but we shall return to the matter again in section 5.1.

The additional many-body broadening of the Hubbard satellites, discussed in section 4.2, is demonstrated clearly in figure 7 where $D(\omega)$ is shown for $\tilde{U} = 6$. Superimposed on the spectrum is the predicted strong-coupling form for the Hubbard satellites, consisting in the flat-band case of Lorentzians with half-width $2\Delta_0$ (and net intensity $\frac{1}{2}$); see equation (4.25). These are seen to reproduce well the 'full' Hubbard bands, whose centres for $\tilde{U} = 6$ are also found to be very close to $\pm(U/2)(1 + 4\Delta_0/\pi U)$, as predicted for the flat-band case in section 4.2. For comparison the simple UHF spectrum is also shown: its deficiencies, even as far as the Hubbard satellites are concerned, are obvious.

We consider now in more detail the low-frequency Kondo resonance. In section 4.1 the theory has been shown to yield correctly the Fermi liquid quasiparticle form, equation (4.20),

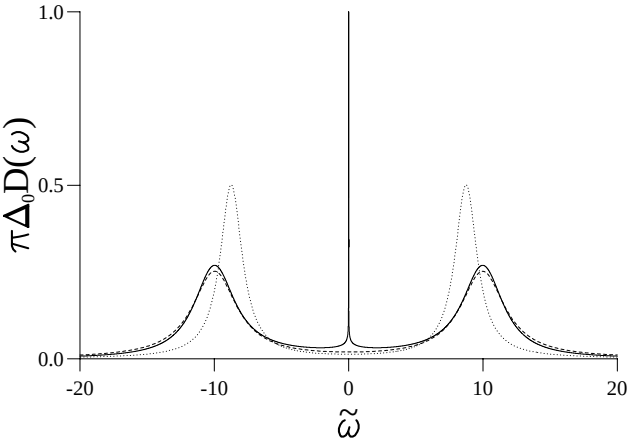

Figure 7. $\pi\Delta_0 D(\omega)$ for the flat-band case with $\tilde{U} = 6$ (solid line), compared to the predicted strong-coupling behaviour of the Hubbard satellites (dashed) and the simple UHF spectrum (dotted).

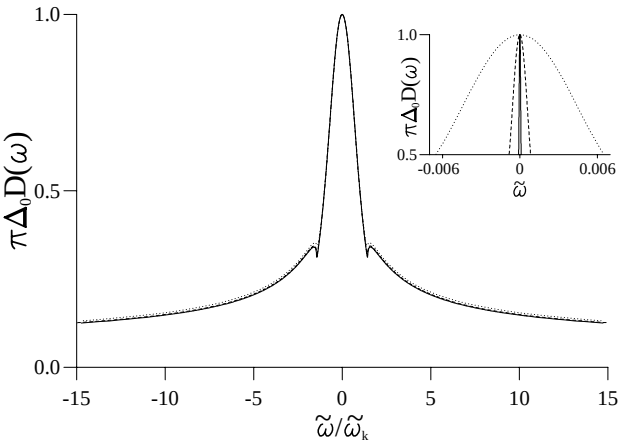

Figure 8. Scaling behaviour of low-energy Kondo resonance: $\pi\Delta_0 D(\omega)$ versus $\tilde{\omega}/\tilde{\omega}_K$ for the flat-band case with $\tilde{U} = 4$ (dotted line), 6 (dashed) and 8 (solid). The small feature at $|\tilde{\omega}/\tilde{\omega}_K| \sim 1.4$ is entirely an artifact of the specific RPA form for Π^{+-}_{AA}: see figure 12. Inset: corresponding $\pi\Delta_0 D(\omega)$ on an 'absolute' scale, to illustrate exponential narrowing of the Kondo resonance in the $\tilde{U}$-range considered.

for $G(\omega)$, with quasiparticle weight $Z \propto \omega_m$ in strong coupling (equation (4.21)), and in terms of which the low-ω behaviour of $D(\omega)$ must (and does) scale universally. Strictly speaking, the quasiparticle form is of course valid for $\tilde{\omega}/Z \ll 1$ (see section 2); and although naive extrapolation of it would imply a pure Lorentzian lineshape with $\tilde{\omega}_K = Z$, scaling solely in terms of $\tilde{\omega}/\tilde{\omega}_K$ for all frequencies, we do not expect either to be true for finite $\tilde{U}$. We do nonetheless expect to see, as $\tilde{U} \to \infty$, the emergence of scaling behaviour that is not confined only to $\tilde{\omega}/\tilde{\omega}_K \ll 1$. To illustrate this, figure 8 shows $\pi\Delta_0 D(\omega)$ for $\tilde{U} = 4$, 6 and 8. The inset shows the central portion of the resonance on an 'absolute' scale, to illustrate its exponential decrease for the $\tilde{U}$s considered. The main figure by contrast shows $\pi\Delta_0 D(\omega)$ versus $\tilde{\omega}/\tilde{\omega}_K$. From this, the scaling behaviour (and non-Lorentzian form)

of $D(\omega)$ is evident; and the expected small finite-U corrections, apparent with increasing $\tilde{\omega}/\tilde{\omega}_K$ and diminishing with increasing $\tilde{U}$, are seen.

Finally, we point out that the apparent small spectral feature occurring in figure 8 at $|\tilde{\omega}/\tilde{\omega}_K| \sim 1.4$ is entirely an artifact of using the specific RPA form for Π^{+-}_{AA} (equation (2.20)) in equation (3.12) for the interaction self-energy. This is examined further in the following section, where a heuristic remedy for it is given.

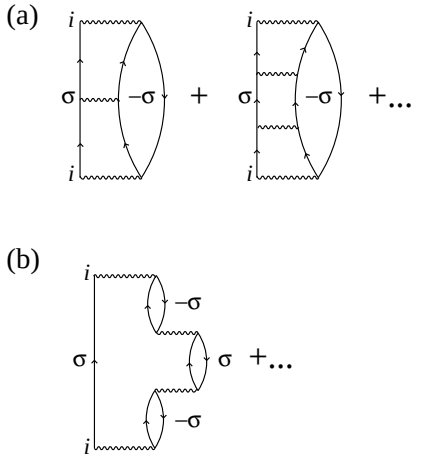

Figure 9. (a) Repeated particle–particle and (b) 'bubble' contributions to $\Sigma_{i\sigma}$.

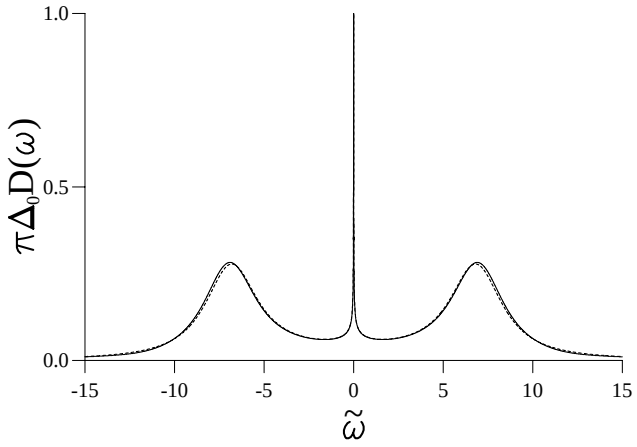

Figure 10. $\pi\Delta_0 D(\omega)$ versus $\tilde{\omega}$ for the flat-band case with $\tilde{U} = 4$, including and omitting particle–particle plus bubble contributions (solid and dashed lines respectively).

5.1. Extensions

The dynamical self-energy diagrams hitherto considered are shown in figure 3; they include repeated particle–hole interactions in the transverse spin channel (leading to the RPA form for Π^{+-}_{AA} occurring in equation (3.10) for $\Sigma_{A\uparrow}$; see also figure 1). It is natural to examine likewise the additional effects of including both repeated particle–particle and 'bubble'

interactions. These are shown in figures 9(a), 9(b) respectively, and to lowest order in U are $\mathcal{O}(U^3)$ and $\mathcal{O}(U^4)$. (The corresponding diagram of order U^2 is already included in figure 3 and equation (3.10).) $\Sigma_{A\uparrow}(\omega)$ is then the sum of figures 3 and 9; the local moment $|\mu|$ is again determined from the pinning condition equation (3.16), and $\tilde{U}_0$ is thereby found to decrease slightly to $\tilde{U}_0 \simeq 0.89$. If one worked with the restricted HF saddle point ($|\mu| = 0$ for all $\tilde{U}$), the sum of repeated bubble diagrams in figure 9(b) suffers for $\tilde{U} \geqslant 1$ from the same divergence and instability as the corresponding transverse spin $\Pi^{+-}_{\alpha\alpha}$, equation (2.26). But with $|\mu| \neq 0$, this behaviour is again eliminated entirely. In fact, neither the particle–particle nor the bubble diagrams make any appreciable contribution to the single-particle spectrum. This is evident from figure 10, which shows $\pi\Delta_0 D(\omega)$ for $\tilde{U} = 4$, with and without the additional contributions. The same situation occurs as $\tilde{U} \to 0$ (as one expects from the higher-order nature of the diagrams) and, while the role of such in relative terms is more significant for $\tilde{U} \sim 1$–2, even here their effects are minor.

There are two essential elements to the theory developed thus far.

(i) First, that $\Sigma_{A\uparrow}$ has a contribution given from figure 3 by the form equation (3.10), capturing the dynamical spin-flip scattering required to describe the Kondo limit, as reflected in particular in the low-frequency resonance in $\mathrm{Im}\,\Pi^{+-}_{AA}(\omega)$.

(ii) That equation (3.16) must be satisfied: $D(\omega = 0)$ is pinned, the Friedel sum rule is satisfied.

The calculations described above have however been more specific in that we have employed the RPA form equation (2.20) for Π^{+-}_{AA}, with bare interaction vertex U, and with equation (3.16) used in practice to determine the local moment $|\mu|$. However this degree of specificity is not in fact necessary, and we now sketch two variants of the basic approach that lead in particular to the same strong-coupling asymptotics.

The first involves a simplified vertex renormalization: the RPA form for Π^{+-}_{AA} is retained, but with the bare interaction U replaced by a renormalized vertex U'; specifically, $\Pi^{+-}_{AA} = {}^0\Pi^{+-}_{AA}/[1 - U'{}^0\Pi^{+-}_{AA}]$. Strictly speaking, vertex renormalization will of course lead to an ω-dependent U'. We merely mimic it phenomenologically, but simply, via a static interaction for which, in a wide range of contexts, there is ample precedent (see e.g. [23]); and, since its use is largely heuristic, we do not specify here the (many) possible diagrammatic resummations to which U' could correspond. In the context of figure 3 for $\Sigma_{A\uparrow}$, the interior U-vertices are thus replaced by U'. Likewise, so too are the two end U-vertices: again, there are many possible classes of resummation for which this is appropriate. Equation (3.10) for $\Sigma_{A\uparrow}(\omega)$ is thus modified to

$$\Sigma_{A\uparrow}(\omega) = [U']^2 \int_{-\infty}^{\infty} \frac{\mathrm{d}\omega_1}{2\pi\,\mathrm{i}}\, \frac{{}^0\Pi^{+-}_{AA}(\omega_1)}{1 - U'{}^0\Pi^{+-}_{AA}(\omega_1)} \mathcal{G}_{A\downarrow}(\omega_1 + \omega) \tag{5.1}$$

where (see section 3.2) ${}^0\Pi^{+-}_{AA}$ and $\mathcal{G}_{A\downarrow}$ again depend parametrically on U and $|\mu|$ only via the combination $x = \frac{1}{2}U|\mu|/\Delta_0$.

The pinning condition, equation (3.16), is now enforced. In direct parallel to equation (3.17), it may be cast as

$$f(U'; x) = x \tag{5.2}$$

where $f(U'; x) = \Delta_0^{-1}\Sigma^{R}_{A\uparrow}(\omega = 0)$. The problem may now be solved in three simple steps.

(a) For any given $x = \frac{1}{2}U|\mu|/\Delta_0$, equation (5.2) is solved for U'.

(b) The single-particle spectrum, given from equations (3.1)–(3.3) by $D(\omega) = \frac{1}{2}[D_{A\uparrow}(\omega) + D_{A\downarrow}(\omega)]$ with $D_{A\downarrow}(\omega) = D_{A\uparrow}(-\omega)$, then follows directly since $\tilde{\Sigma}_{A\uparrow}(\omega) =$

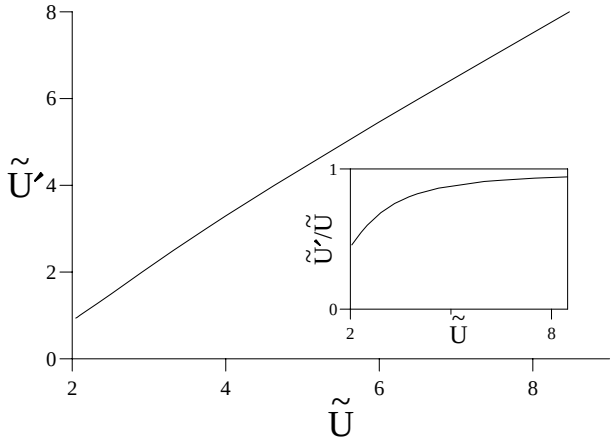

Figure 11. $\tilde{U}' = U'/\pi\Delta_0$ versus $\tilde{U}$, as explained in the text. Inset: $\tilde{U}'/\tilde{U}$ versus $\tilde{U}$.

$-\frac{1}{2}U|\mu| + \Sigma_{A\uparrow}(\omega)$ depends parametrically only on U' and x. From this, the local moment $|\mu|$ is then determined via

$$|\mu| = \int_{-\infty}^{0} d\omega\, [D_{A\uparrow}(\omega) - D_{A\downarrow}(\omega)] \tag{5.3}$$

(which is thus satisfied self-consistently).

(c) Since $x = \frac{1}{2}U|\mu|/\Delta_0$ is specified, and $|\mu|$ is now known, U follows directly. In this way one obtains the $\tilde{U} = U/\pi\Delta_0$ dependence of $\tilde{U}' = U'/\pi\Delta_0$, $|\mu|$ and the impurity spectrum; and for the flat-band case the resultant $\tilde{U}$-dependence of $\tilde{U}'$ is shown in figure 11.

The solution to the approach just outlined is in fact already contained in the results from the theory pursued in the preceding sections. The reason for this is that $\Sigma_{A\uparrow}$ in the latter approach (equation (5.1)) depends parametrically on U' and x in precisely the same way that $\Sigma_{A\uparrow}$ in the original approach (equation (3.10) with (2.20)) depends on U and x. In particular, the function $f(y; x)$ appearing in equation (5.2) with $y = U'$ is precisely the same function arising in equation (3.17) with $y = U$; and once either equation (3.17) or equation (5.2) as appropriate is solved, the single-particle spectrum follows directly. Hence the impurity spectrum obtained in the original approach for any given $U = a > U_0$ is precisely that appropriate to the latter approach with $U' = a$, and the corresponding U is then obtained from figure 11: the spectra shown in figure 4, for example, now correspond to $\tilde{U}' = 6, 4$ and 2.5 and hence from figure 11, to $\tilde{U} \simeq 6.5$, 4.6 and 3.3. Further, as illustrated in the inset to figure 11, $\tilde{U}'/\tilde{U} \sim 1 - \mathcal{O}(\tilde{U}^{-1})$ as $\tilde{U} \to \infty$. This, coupled with the corresponding asymptotic behaviour $|\mu| \sim 1 - \mathcal{O}(\tilde{U}^{-1})$, is readily shown to be sufficient to ensure that the leading strong-coupling behaviours of the two approaches coincide, in particular equation (4.11) for the Kondo scale and the scaling (figure 8) of the Kondo resonance.

In fact, as figure 11 shows, the latter approach amounts in practice to a simple elongation of the $\tilde{U}$-axis in the original approach. As such, it has the advantage of not suggesting the persistence of essentially strong-coupling behaviour down to somewhat too low values of $\tilde{U}$ (as found with the original approach). But it does have an obvious disadvantage in that $\tilde{U}'$ is simply undetermined for $\tilde{U}' < \tilde{U}'_0 \simeq 0.94$ (i.e. $\tilde{U} < 2.04$ from figure 11): below this value, $|\mu| = 0$ and hence $x = 0$, and for $x = 0$ equation (5.2) is trivially satisfied for any $\tilde{U}' < \tilde{U}'_0$. This is largely a reflection of our phenomenological use of U': to

ensure a smooth passage to the non-interacting limit—as occurs naturally in the original approach—obviously requires a specific theory for U' itself, a matter we pursue no further here.

The second extension we consider is motivated by the fact that the two key elements of the basic theory, specified as (i) and (ii) above, do not require Π^{+-}_{AA} occurring in equation (3.10) for $\Sigma_{A\uparrow}$ to be given by the RPA form equation (2.20). In particular, neither the strong-coupling asymptotics deduced in section 4, nor the low-frequency behaviour established in section 3.2, require Π^{+-}_{AA} to be thus given. The specific calculations leading to figures 4–8 have, however, employed Π^{+-}_{AA} in RPA form. From equation (2.34*a*) it follows that while the resonance in the resultant $\mathrm{Im}\,\Pi^{+-}_{AA}(\omega)$ is indeed *centred* on $\omega = \omega_m$, its effective *width* in strong coupling is of order $\omega_m/\tilde{U}^2$. And this in turn may be shown to underlie the small spectral feature occurring in the strong-coupling scaled spectrum (figure 8) at $\tilde{\omega}/\tilde{\omega}_K \sim 1.4$, which is thus an artefact of employing the specific RPA form.

In a more elaborate theory, however, we anticipate that in strong coupling $\mathrm{Im}\,\Pi^{+-}_{AA}(\omega)$ may have both its maximum *and* width of the order of the Kondo scale ω_m, i.e. that it takes the form

$$\frac{1}{\pi}\mathrm{Im}\,\Pi^{+-}_{AA}(\omega) = \frac{1}{\omega_m}F(\omega/\omega_m). \tag{5.4}$$

Subject only to

$$\int_0^\infty \frac{d\omega}{\pi}\ \mathrm{Im}\,\Pi^{+-}_{AA}(\omega) \sim 1$$

as $\tilde{U} \to \infty$ (see equation (4.2)), such a form again leads naturally to the same exponential asymptotics for ω_m (equation (4.11)); to the quasiparticle form equation (4.20) for the low-ω behaviour of $G(\omega)$; and to the same strong-coupling asymptotics (section 4.2) for the Hubbard satellites.

Our aim now is simply to show that the form equation (5.4) indeed eliminates the small spectral anomaly in figure 8. To this end, and purely for illustrative purposes, we consider an $F(y)$ of the form

$$F(y) = A\frac{y}{1+y^2}e^{-y/\alpha} \tag{5.5}$$

for $y > 0$, and zero for $y < 0$. The spectral weight of $\mathrm{Im}\,\Pi^{+-}_{AA}(\omega)$ is thus confined to frequencies $\omega > 0$, as appropriate in strong coupling (see equation (4.2)); the constant A is determined from

$$\int_0^\infty \frac{d\omega}{\pi}\ \mathrm{Im}\,\Pi^{+-}_{AA}(\omega) = 1$$

and the constant α, chosen quite arbitrarily such that $\alpha \gg 1$, merely serves as a high-frequency cut-off to ensure the resonance is normalizable. The specific form of $F(y)$ should not of course be taken too seriously, but it serves to illustrate the point, since the maximum of $F(y)$ occurs for $y = 1 + \mathcal{O}(1/\alpha)$ and its effective width is likewise of order unity. Equations (5.4), (5.5) for $\mathrm{Im}\,\Pi^{+-}_{AA}$ are now employed in the basic expression equation (3.12) for the self-energy $\Sigma_{A\uparrow}(\omega)$; and for simplicity the local moment $|\mu|$ in both $\mathcal{G}_{A\downarrow}$ and $\tilde{\Sigma}_{A\uparrow}$ (equation (3.9)) is set to its UHF value $|\mu_0|$.

The modelling is not solely engineering however, since for given $\tilde{U}$, ω_m must now be determined from the pinning condition equation (3.16) (in which way we confirm explicitly that equation (4.11) for the Kondo scale is correctly recovered). For the flat-band case, and in direct analogy to figure 8, figure 12 shows the resultant low-ω behaviour of the Kondo

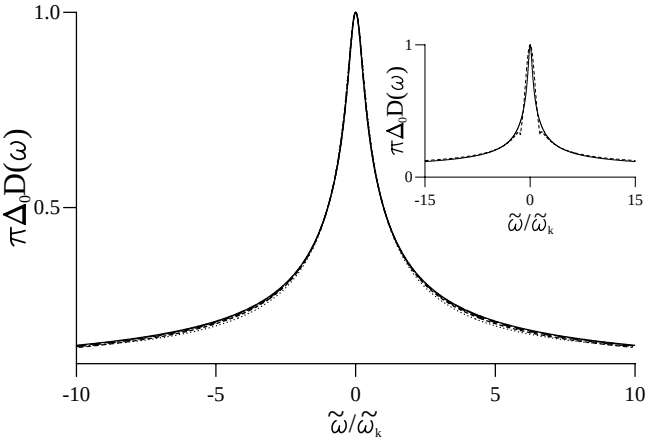

Figure 12. Low-energy scaling behaviour of $D(\omega)$ as explained in the text: $\pi\Delta_0 D(\omega)$ versus $\tilde{\omega}/\tilde{\omega}_K$ for $\tilde{\omega}_m = \omega_m/\Delta_0 = 10^{-m}$ with $m = 1$–5 ($m = 5$ is the solid line), corresponding respectively to $\tilde{U}$ ranging from ∼5–11. Inset: Comparison of scaling form (solid line) to that shown in figure 8 (dashed line).

resonance: $\pi\Delta_0 D(\omega)$ versus $\tilde{\omega}/\tilde{\omega}_K$ (with $\tilde{\omega}_K \propto \tilde{\omega}_m$ again the half-width at half-maximum of the resonance) for $\tilde{\omega}_m = 10^{-m}$ with $m = 1$–5, corresponding respectively to $\tilde{U}$ ranging from around 5 to 11. The scaling behaviour is clear; and relative to figure 8, a slight redistribution of intensity in the Kondo resonance has occurred (as illustrated further in the inset to figure 12), which indeed eliminates the spectral anomaly.

6. Summary

We have described in this paper a rather simple, yet inherently non-perturbative, approach to single-particle spectra of the symmetric Anderson model. By introducing local moments explicitly from the outset, and employing a two-self-energy description that captures in a physically transparent fashion the dynamical spin-flip scattering essential to the spin-fluctuation limit, the resultant theory transcends quite successfully a number of limitations of previous approaches: it covers simultaneously both low- and high-energy excitations—the Kondo resonance and Hubbard satellites—while preserving correctly Fermi liquid behaviour at low energies; it encompasses the strong-coupling behaviour of the spectrum on both low- and high-energy scales, while in weak coupling it is perturbatively exact to second order in U; and the atomic limit is also correctly recovered. Imposition of the Friedel sum rule—whereby the single-particle spectrum at a single point, the Fermi level $\omega = 0$, is pinned at its non-interacting value—underlies to a large extent the essential success of the method: its imposition, as a self-consistency condition, in particular leads non-trivially to both the emergence of Fermi liquid behaviour at low energies and the asymptotics of the Kondo scale in strong coupling, where the exponential dependence of the latter, known [2] e.g. from scaling and the Bethe *ansatz*, is correctly recovered. Further, while a flat-band host has latterly been employed for tangible illustration of spectra, the theory is not of course restricted to this special case; it can deal readily with a more realistic hybridization function, where the requisite computations are straightforward and rapid.

Finally, and importantly, we add that the underlying approach is not confined to the description of a Fermi liquid state, but can also handle an insulating or semi-metallic host

where use of a two-self-energy description is in general a necessity and not a luxury; this, as well as extension of the present work to finite temperatures, will be described in subsequent publications.

Acknowledgments

DEL expresses his warm thanks to Ph Nozières for the hospitality of the Institut Laue–Langevin, Grenoble. We are also deeply grateful to the many people with whom we have had stimulating discussions regarding the present work. MPE acknowledges an EPSRC studentship, and we are further grateful to the EPSRC (Condensed Matter Physics) for financial support.

Appendix

The polarization bubble (diagram (a), figure 1) is given by equation (2.18), with the bare propagators from equation (2.12). For the flat-band case, with $\Delta_{\mathrm{I}}(\omega) = \Delta_0$ and $\Delta_{\mathrm{R}}(\omega) = 0$, ${}^0\Pi^{+-}_{\mathrm{AA}}$ may be obtained in closed form. With $\tilde{\omega} = \omega/\Delta_0$ and $x = \frac{1}{2}U|\mu|/\Delta_0 = \tilde{U}|\tilde{\mu}|$, the result is

$$\begin{aligned}\pi\Delta_0\,\mathrm{Re}\,{}^0\Pi^{+-}_{\mathrm{AA}}(\omega) = {} & \frac{1}{2x-\tilde{\omega}}\left[\tan^{-1}(x)+\tan^{-1}(x-\tilde{\omega})\right] \\ & + \frac{(2x-\tilde{\omega})}{(2x-\tilde{\omega})^2+4}\left[\tan^{-1}(x)-\tan^{-1}(x-\tilde{\omega})\right] \\ & + \frac{1}{(2x-\tilde{\omega})^2+4}\ln\left[\frac{(x^2+1)}{(x-\tilde{\omega})^2+1}\right] \end{aligned} \tag{A.1}$$

and

$$\begin{aligned}\pi\Delta_0\,\mathrm{Im}\,{}^0\Pi^{+-}_{\mathrm{AA}}(\omega) = {} & \mathrm{sgn}(\tilde{\omega})\,\frac{2}{(2x-\tilde{\omega})^2+4} \\ & \times\left\{\frac{1}{(2x-\tilde{\omega})}\ln\left[\frac{(x^2+1)}{(x-\tilde{\omega})^2+1}\right]+\tan^{-1}(x)-\tan^{-1}(x-\tilde{\omega})\right\}\end{aligned} \tag{A.2}$$

(such that $\mathrm{Im}\,{}^0\Pi^{+-}_{\mathrm{AA}}(\omega) \geqslant 0\ \forall\tilde{\omega}$). The remaining ${}^0\Pi_{\alpha\alpha}$s follow by symmetry from equations (2.19).

References

[1] Anderson P W 1961 *Phys. Rev.* **124** 41
[2] Hewson A C 1993 *The Kondo Problem to Heavy Fermions* (Cambridge: Cambridge University Press)
[3] Tsvelik A M and Wiegmann P B 1983 *Adv. Phys.* **32** 453
Schlottmann P 1989 *Phys. Rep.* **181** 1
[4] Krishnamurthy H R, Wilkins J W and Wilson K G 1980 *Phys. Rev.* B **21** 1003
Krishnamurthy H R, Wilkins J W and Wilson K G 1980 *Phys. Rev.* B **21** 1044
[5] Gunnarsson O and Schönhammer K 1983 *Phys. Rev.* B **28** 4315
[6] Gunnarsson O and Schönhammer K 1985 *Phys. Rev.* B **31** 4815
[7] Bickers N E, Cox D L and Wilkins J W 1987 *Phys. Rev.* B **36** 2036
[8] Kuramoto Y 1983 *Z. Phys.* B **53** 37
[9] Keiter H and Kimball J C 1971 *Int. J. Magn.* **1** 233
Keiter H and Morandi G 1984 *Phys. Rep.* **109** 227
[10] Bickers N 1987 *Rev. Mod. Phys.* **59** 845
[11] Pruschke Th and Grewe N 1989 *Z. Phys.* B **74** 439
[12] Read N and Newns D M 1983 *J. Phys. C: Solid State Phys.* **16** 3273

Read N and Newns D M 1983 *J. Phys. C: Solid State Phys.* **16** L1055
[13] Coleman P 1987 *Phys. Rev.* B **35** 5072
[14] Holm J, Kree R and Schönhammer K 1993 *Phys. Rev.* B **48** 5077
[15] Yosida K and Yamada K 1970 *Prog. Theor. Phys. Suppl.* **46** 224
Yamada K 1975 *Prog. Theor. Phys.* **53** 970
Yamada K 1976 *Prog. Theor. Phys.* **55** 1345
[16] Horvatić B and Zlatić V 1985 *Solid State Commun.* **54** 957
Horvatić B, Šokčević D and Zlatić V 1987 *Phys. Rev.* B **36** 675
[17] White J A 1992 *Phys. Rev.* B **45** 1100
[18] Hewson A C 1966 *Phys. Rev.* **144** 420
[19] Thouless D J 1972 *The Quantum Mechanics of Many-Body Systems* (New York: Academic)
[20] Anderson P W 1970 *J. Phys. C: Solid State Phys.* **3** 2436
[21] Nozières P 1974 *J. Low Temp. Phys.* **17** 31
[22] See e.g.
Hewson A C 1993 *The Kondo Problem to Heavy Fermions* (Cambridge: Cambridge University Press) p 113
[23] Bickers N E and White S R 1991 *Phys. Rev.* B **43** 8044
Bulut N, Scalapino D J and White S R 1993 *Phys. Rev.* B **47** 2742
Doré A-M, Chen L and Tremblay A-M S 1994 *Phys. Rev.* B **49** 4106